
Topological Order in Quantum N -mer Models

Submitted by
Sven Jandura



BACHELOR THESIS

Faculty of Physics

Ludwig Maximilians Universität München

Supervisor

Prof. Dr. Jan von Delft

June 06, 2019

Topologische Ordnung in Quanten N -mer Modellen

Vorgelegt von
Sven Jandura



BACHELORARBEIT

Fakultät für Physik

Ludwig Maximilians Universität München

Betreuer

Prof. Dr. Jan von Delft

06. Juni 2019

Abstract

In this thesis I study Quantum N -mer models, a natural generalization of quantum dimer models. I show how Quantum N -mer models can be formulated using the language of tensor networks and give a description of their ground state. I prove that the ground space of the trimer model on the kagome lattice is exactly nine-fold degenerated. Furthermore I give numerical evidence suggesting that the trimer model on the kagome lattice does not exhibit topological order and construct a similar model which does. Finally I also give a mapping from the dimer model on the square lattice to a model of oriented loops, which is more intuitive in some situations.

Zusammenfassung

In dieser Arbeit untersuche ich Quanten N -mer Modelle, eine natürliche Verallgemeinerung von Quanten Dimermodellen. Ich zeige wie sich Quanten N -mer Modelle mithilfe von Tensor Netzwerken ausdrücken lassen und wie sich ihr Grundzustand beschreiben lässt. Ich beweise dass der Grundzustand des Trimermodells auf dem Kagomegitter genau neunfach entartet ist. Des weiteren präsentiere ich numerische Evidenz dafür, dass das Trimermodell auf dem Kagomegitter keine topologische Ordnung aufweist. Ich konstruiere außerdem ein ähnliches Modell, welches dies doch tut. Schlussendlich zeige ich dass das Dimermodell auf dem Quadratgitter äquivalent zu einem Modell gerichteter Schleifen ist, welches in machen Situationen intuitiver erscheint.

Contents

| | | |
|----------|---|-----------|
| 1 | Introduction | 1 |
| 2 | Introduction to Tensor Networks | 2 |
| 2.1 | Graphs on a Torus | 2 |
| 2.2 | Definition of Tensor Networks | 4 |
| 2.3 | Parent Hamiltonians | 6 |
| 2.4 | Correlation Length | 11 |
| 3 | Quantum N-mer Models | 14 |
| 3.1 | Quantum N-mer Models as Tensor Networks | 14 |
| 3.2 | Ground States of Constraint Models | 18 |
| 3.3 | Topological Invariants | 21 |
| 4 | The Trimer Model on the Kagome Lattice | 24 |
| 4.1 | From Kagome to Honeycomb Lattice | 24 |
| 4.2 | Blocking Tensors on the Honeycomb Lattice | 27 |
| 4.3 | From Honeycomb to Triangular Lattice | 30 |
| 4.4 | Topological Order | 33 |
| 4.4.1 | A Simple Example | 33 |
| 4.4.2 | Topological Order in the Trimer Model on the Kagome Lattice . . | 35 |
| 5 | The Dimer Model on the Square Lattice | 39 |
| 6 | Conclusion | 43 |

1 Introduction

Toy models, which are deliberately simplified models aiming to explain the essential physics of a phenomenon, have a long history in the study of quantum systems. A well known example of such toy models, describing the basic properties of ferromagnets and antiferromagnets, is the Ising model [1]. Another such toy model is the quantum dimer model, first introduced by Rokhsar and Kivelson in 1988 [2] to study high temperature superconductivity. While it turned out that the quantum dimer model is not a good description for the ground state of high temperature superconductors, it has many other remarkable properties.

In particular, it has been noted by Moessner and Sondhi [3] that there are exactly four orthogonal ground states of the quantum dimer model on a triangular lattice. However, these ground states cannot be distinguished by only looking at lattice sites in some small region, we actually have to look at lattice sites everywhere on the lattice. This implies that the model exhibits topological order, a property first described by Wen [4], which has been extensively studied by another famous toy model, Kitaev's toric code [5]. Topological models have many interesting properties, for example the existence of anyons, which are quasiparticles obeying neither bosonic nor fermionic statistics.

A natural generalization of the quantum dimer model is the quantum trimer model, which has been studied in [6], and general quantum N -mer models. They will be the object of study in this thesis.

This thesis starts with an introduction to the language of tensor networks in section 2. Tensor networks are a useful way to describe interesting quantum states on a lattice. They also allow to formulate a Hamiltonian such that the studied quantum state is a ground state of that Hamiltonian. Furthermore, they can be used to calculate the correlation length of the described state. In section 3 I define general quantum N -mer models and show how they can be described by a tensor network. This is the first part of original work in this thesis. I also give a characterization of the ground state of quantum N -mer models in terms of moves of N -mers on the lattice, and show that these moves must conserve certain invariants. In section 4 I study the special case of the trimer model on the kagome lattice. In sections 4.1 - 4.3 I give a rigorous proof that the ground space of this model is exactly nine-fold degenerated. In section 4.4 I then give evidence that even though this degeneracy depends on the genus of the surface the state lives on, the model does not exhibit topological order. However, I show that we can modify the model slightly, so that it does exhibit topological order. In section 5 I then study the original dimer model on the square lattice and show that it is equivalent to a model of oriented loops. This gives a better intuition for the ground state degeneracy of this model. Section 4 and 5, with exception of the introduction to topological order in section 4.4.1, are original work.

2 Introduction to Tensor Networks

We start this thesis in section 2.1 by defining graphs and their basic properties, which will be useful when studying quantum states that live on graphs. We will then define tensor networks and projected entanglement pair states (PEPS) in section 2.2 and construct a Hamiltonian such that a given PEPS is the ground state of that Hamiltonian in section 2.3. Finally in section 2.4 we will derive correlation length of a PEPS.

2.1 Graphs on a Torus

In this thesis we consider quantum states that live on a lattice. As a lattice is just a special kind of graph, we need some notations from graph theory.

Definition 2.1 (Graph, Directed Graph, Directed Graph with Half Edges).

Let V and E be finite sets. We will call the elements of V vertices and the elements of E edges.

1. Let $S \subseteq V \times E$ such that for each $e \in E$ there are exactly two vertices $v_1, v_2 \in V$ such that $(v_1, e), (v_2, e) \in S$. The triple $G = (V, E, S)$ is called a graph. The edge e is said to connect the vertices v_1 and v_2 .
2. Let $\text{START} : E \rightarrow V$ and $\text{END} : E \rightarrow V$ be two functions. The quadruple $G = (V, E, \text{START}, \text{END})$ is called a directed graph. And edge e is said to start in $\text{START}(e)$ and to end in $\text{END}(e)$.
3. Let $\text{START}, \text{END} \subseteq V \times E$ such that for all $e \in E$ there is (a) a $v \in V$ with $(v, e) \in \text{START}$ or $(v, e) \in \text{END}$, (b) at most a one $v_s \in V$ such that $(v_s, e) \in \text{START}$ and (c) at most one $v_e \in V$ such that $(v_e, e) \in \text{END}$. The quadruple $G = (V, E, \text{START}, \text{END})$ is called a directed graph with half edges. Edges e such that there are $v_1, v_2 \in V$ with $(v_1, e) \in \text{START}$ and $(v_2, e) \in \text{END}$ are called full edges. Edges that are not full edges are called half edges.

Remark 2.2.

1. Oftentimes we will just write $G = (V, E)$ and leave the relation between the vertices and edges implicit.
2. Each directed graph has an (undirected) graph associated with it.
3. A directed graph is a special case of a directed graph with half edges. The generalization of a graph with half edges in which an edge can join any number of vertices is called a hypergraph.

Directed graphs in which any two vertices are connected by at most one edge can also conveniently be represented as a pair (V, E) where the edges $E \subseteq V \times V$ are just ordered pairs of vertices. We get our original definition by letting START map an edge (v_1, v_2) to v_1 , and letting END map (v_1, v_2) to v_2 . We will often use this description of a directed graph.

Given a directed graph or a directed graph with half edges, we can define a subgraph:

Definition 2.3 (Subgraph). Let $G = (V, E, \text{START}, \text{END})$ be a directed graph with half edges, and let $V' \subseteq V$ and $E' = \{e \in E | e \text{ is connected to a } v \in V'\}$. The directed graph with half edges $G' = (V', E', \text{START}', \text{END}')$ given by $\text{START}' = \{(v, e) \in \text{START} | v \in V'\}$ and $\text{END}' = \{(v, e) \in \text{END} | v \in V'\}$ is called a subgraph of G .

The vertices of all graphs in this thesis will be a subset of the torus:

Definition 2.4 (Torus). Let $r, s \in \mathbb{R}$. $\mathbb{T}_{r,s} = \mathbb{R}^2 / \sim$ with $x \sim y \Leftrightarrow \exists n, m \in \mathbb{N} : x - y = (nr, ms)$ for all $x, y \in \mathbb{R}^2$ is called the torus with side lengths r and s .

In this thesis we will mainly need the square-, kagome-, honeycomb-, and triangular lattice. These graphs are shown in Figure 1.

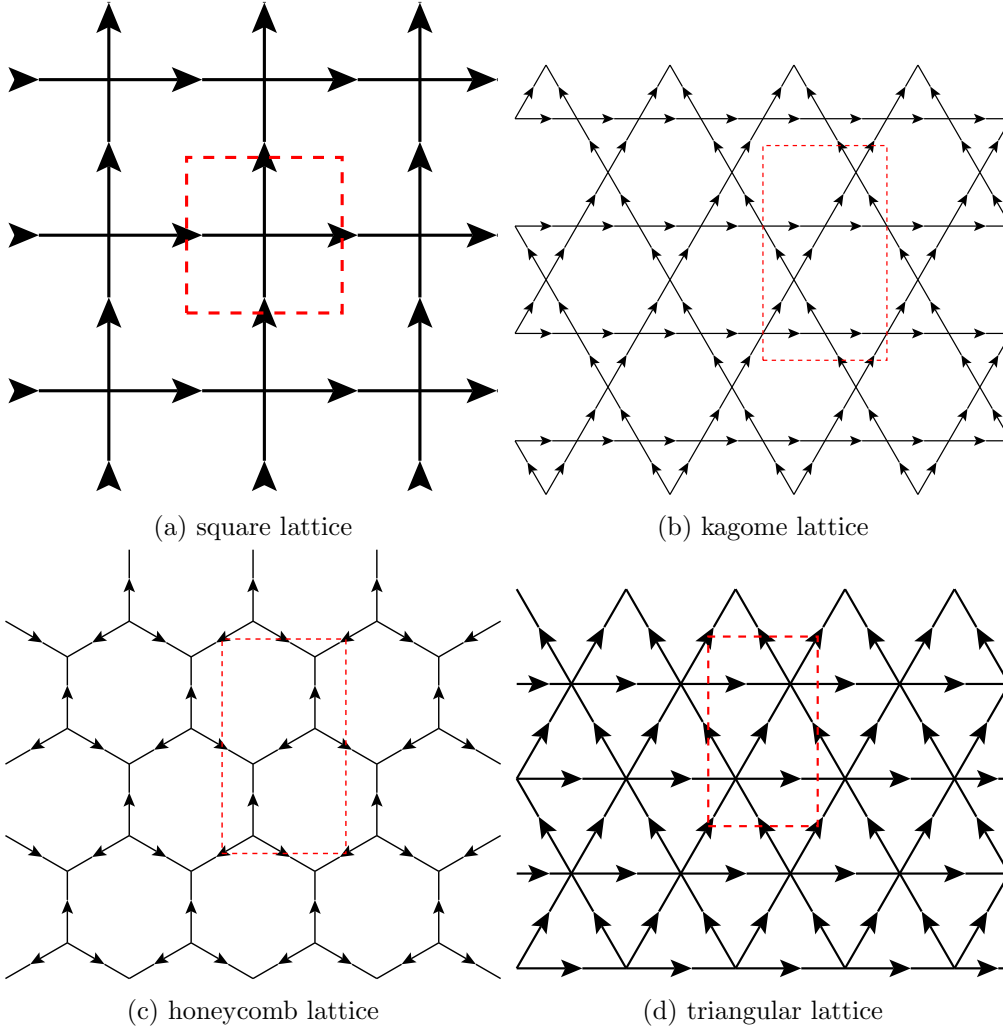


Figure 1: The four lattices we will mainly consider. The dashed rectangle shows a rectangular unit cell. A N_x, N_y -lattice consists of N_x of these cells in the x -direction, and N_y of those cells in the y -direction.

For all of these graphs we can define their faces and their dual graphs.

Definition 2.5 (Faces of a Graph, Dual Graph). Let $G = (V, E)$ be a directed graph and $V \subseteq \mathbb{T}_{r,s}$ for $r, s \in \mathbb{R}$

1. The connected components (in the quotient topology) of

$$\mathbb{T}_{r,s} \setminus \{tv_1 + (1-t)v_2 | t \in [0, 1], v_1 \text{ and } v_2 \text{ connected by an edge}\}$$

are called the faces of G .

2. Two faces F_1 and F_2 are said to border each other, if $\partial F_1 \cap \partial F_2 = \{tv_1 + (1-t)v_2 | t \in [0, 1]\}$ for an edge connecting the vertices v_1 and v_2 .
3. The graph whose vertices are given by the faces of G and whose edges are the pairs of bordering faces of G is called the dual graph of G .

We will frequently consider paths on a graph.

Definition 2.6 (Path on a Graph). Let $G = (V, E)$ be a graph.

1. A n -tuple $\gamma = (v_1, v_2, \dots, v_n) \in V^n$ ($n \in \mathbb{N}$) such that there is an edge that connects v_i and v_{i+1} for $i = 1, \dots, n-1$ is called a path.
2. If $v_1 = v_n$, γ is called a closed path on G .

For a closed path of the dual graph of some graph we can define its winding number:

Definition 2.7 (Winding Number). Let G be a graph with vertices in $\mathbb{T}_{r,s}$ ($r, s \in \mathbb{R}$) and G' its dual graph. Let $\gamma = (v_1, \dots, v_n)$ ($n \in \mathbb{N}$) be a closed path in G' . We can construct a path $\tilde{\gamma}$ on $\mathbb{T}_{r,s}$ by choosing a point x_i in each face v_i in γ and choosing $x_1 = x_n$. For $i = 1, \dots, n-1$ we can choose a path $\tilde{\gamma}_i$ from x_i to x_{i+1} such that the edge in G between the faces v_i and v_{i+1} is the only edge being intersected by $\tilde{\gamma}_i$. We then set $\tilde{\gamma}$ to be the junction of $\tilde{\gamma}_1, \dots, \tilde{\gamma}_{n-1}$. The winding numbers (W_x, W_y) of $\tilde{\gamma}$ are called the winding numbers of γ .

Remark 2.8. The winding numbers of γ don't depend on the choice of $\tilde{\gamma}$, because there is clearly a homotopy between any two paths on the torus we could have chosen.

2.2 Definition of Tensor Networks

Tensor networks are a useful language to describe quantum states on that live on a lattice. Tensor networks can be used as an analytic tool, as well as for numerical simulation techniques for quantum many body systems, like density matrix renormalization group (DMRG) [7] and time-evolving block decimation (TEBD) [8]. For a comprehensive review of applications of tensor networks see [9] and [10].

Tensor networks can be best explained using an example: Suppose we have five inner product spaces \mathcal{H}_i , $i = 1, 2, \dots, 5$. Denote by \mathcal{H}_i^* the dual space of \mathcal{H}_i . Suppose we have tensors $A \in \mathcal{H}_1 \otimes \mathcal{H}_2^* \otimes \mathcal{H}_3^*$, $B \in \mathcal{H}_2 \otimes \mathcal{H}_4^*$ and $C \in \mathcal{H}_3 \otimes \mathcal{H}_5^*$. Now we can calculate $\text{tr}_2(A \otimes B) \in \mathcal{H}_1 \otimes \mathcal{H}_4^* \otimes \mathcal{H}_3^*$, where we take the partial trace over the vector space \mathcal{H}_2 . Now we can further calculate $\text{tr}_3(\text{tr}_2(A \otimes B) \otimes C) \in \mathcal{H}_1 \otimes \mathcal{H}_4^* \otimes \mathcal{H}_5^*$, where we take the new trace over the vector space \mathcal{H}_3 . This calculation can be described by a directed graph with half edges: Each tensor corresponds to a vertex, and each vector space to a full edge or half edge. The edge associated to the vector space ends in the tensor where the dual of the vector space appears, and starts in the tensor where the vector space appears. The graph for this example is shown in Figure 2. This construction is called a tensor network.

Definition 2.9 (Tensor Network).

1. Let $G = (V, E)$ be a directed graph with half edges. Let $(\mathcal{H}_e)_{e \in E}$ be a family of finite dimensional inner product spaces, and let for $v \in V$ $T_v \in \mathcal{H}_{e_1} \otimes \dots \otimes \mathcal{H}_{e_n} \otimes \mathcal{H}_{f_1}^* \otimes \dots \otimes \mathcal{H}_{f_m}^*$ be a tensor, where e_1, \dots, e_n are the edges starting in v and f_1, \dots, f_m the edges ending in v . The triplet $(G, (\mathcal{H}_e)_e, (T_v)_v)$ is called a tensor network.

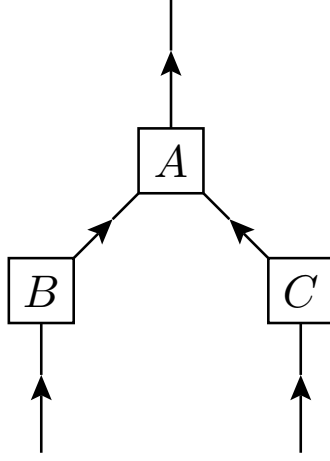


Figure 2: A simple example of a tensor network

- Let E_s be the set of half edges that have a start but no end, and E_e the set of half edges that have an end but no start. Then

$$\text{tr}_{e_1}(\text{tr}_{e_2}(\dots \text{tr}_{e_n}(\bigotimes_{v \in V} T_v) \dots)) \in \bigotimes_{e \in E_s} \mathcal{H}_e \otimes \bigotimes_{e \in E_e} \mathcal{H}_e^*$$

where the traces are taken over all vector spaces $\mathcal{H}_{e_1}, \dots, \mathcal{H}_{e_n}$ where e_1, \dots, e_n are the full edges of G , is called the value of the tensor network.

Remark 2.10.

- The order in which we take the traces is irrelevant. To see this, let \mathcal{H}_1 and \mathcal{H}_2 be two inner product spaces, and $u \in \mathcal{H}_1$, $v \in \mathcal{H}_2$, $\omega \in \mathcal{H}_1^*$ and $\eta \in \mathcal{H}_2^*$. Then

$$\text{tr}_1(\text{tr}_2(u \otimes v \otimes \omega \otimes \eta)) = \text{tr}_1(\eta(v)u \otimes \omega) = \eta(v)\omega(u) = \text{tr}_2(\text{tr}_1(u \otimes v \otimes \omega \otimes \eta))$$

Because traces are linear, the order of the traces does not matter for all arguments.

- We will often denote the value of a tensor network by just drawing the corresponding picture, like Figure 2.

We can now formulate well known theorems from linear algebra in the language of tensor networks. For example

Lemma 2.11 (Completeness Relation). *Let \mathcal{H} be a finite dimensional inner product with dimension d and let x_1, \dots, x_d be a basis of \mathcal{H} and x_1^*, \dots, x_d^* the corresponding dual basis of \mathcal{H}^* . Then*

$$\sum_{i=1}^d \boxed{x_i} \rightarrow \otimes \rightarrow \boxed{x_i^*} = \rightarrow \boxed{\text{id}} \rightarrow$$

where we attach \mathcal{H} to each edge.

Proof. This is just the completeness relation $\sum_{i=1}^d x_i \otimes x_i^* = \text{id}$ written in tensor network notation. \square

Now we can use tensor networks to describe quantum states. Let \mathcal{H}_{phys} and \mathcal{H}_{virt} be two finite dimensional inner product spaces. Given a directed graph $G = (V, E)$ we can extend it to a directed graph with half edges G' by adding a half edge for

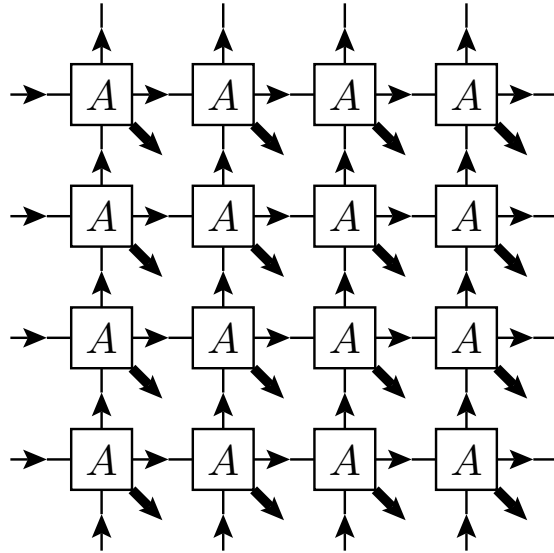


Figure 3: Part of a PEPS on the square lattice on the torus. The physical spaces are shown with bold arrows.

each vertex, starting in this vertex. Now we choose \mathcal{H}_{virt} as the vector space for each full edge in G , and \mathcal{H}_{phys} for each of the newly added half edges. Given a tensor $A_v \in \mathcal{H}_{virt}^{\otimes n} \otimes \mathcal{H}_{virt}^{*\otimes m} \otimes \mathcal{H}_{phys}$, where n is the number of edges starting in a vertex v and m is the number of edges ending in v , the tensor network given by G' , \mathcal{H}_{virt} and \mathcal{H}_{phys} , and $(A_v)_v$ has a value in $\mathcal{H}_{phys}^{\otimes |V|}$. This describes a quantum state with a degree of freedom, for example a spin, on each vertex of the graph. Because \mathcal{H}_{phys} describes the individual degree of freedom it is called the physical space. As we don't see \mathcal{H}_{virt} anymore in the quantum state, it is called the virtual space. If the graph is a 1D-lattice, the state is called a matrix product state (MPS), if the graph is a 2D-lattice, the state is called a projected entanglement pair state (PEPS). An example for such a state on a square lattice where all A_v are the same is shown in Figure 3.

It is nontrivial why we should be able to describe important quantum states using tensor networks. However, it has been shown by Hastings [11] that for 1D-systems the ground state of a gapped, local Hamiltonian can always be approximated by a MPS. Under certain stronger, but physically reasonable, assumptions, the same statement has been shown for PEPS [12]. Another example of a class of quantum states, namely quantum N -mer states, that can be described by a tensor network is given in section 3.

2.3 Parent Hamiltonians

The most straightforward way to study a quantum system is to write down its Hamiltonian and then find its eigenstates, in particular the ground state. However, this procedure is oftentimes way too complicated to be practical. Instead, we can sometimes go the reverse way: We start with a state which has some desired properties (for example given by an experiment) and then construct a Hamiltonian such that the state is the ground state of this Hamiltonian. While this exact Hamiltonian might not be realized in nature, it captures the essential physics leading to the properties of the initial state,

Consider the PEPS $\psi \in \mathcal{H}_{phys}^{\otimes N_x N_y}$ on the N_x, N_y -square lattice given by the tensor network in Figure 3. We want to find a local Hamiltonian operator H such that ψ is a ground state of H . By local we mean that H can be written as $H = \sum_{i=1}^n h_i$ for some $n \in \mathbb{N}$ and

operators h_i which act nontrivially only on a few vertices, that is, there is a hermitian operator $\tilde{h}_i : \mathcal{H}_{phys}^m \rightarrow \mathcal{H}_{phys}^m$ with m much smaller than $N_x N_y$ and $h_i = \tilde{h}_i \otimes \text{id}_{\mathcal{H}_{phys}^{\otimes N_x N_y - m}}$ up to reordering of the factors in the tensor product.

We can find such a Hamiltonian using the construction in [13]:

Theorem 2.12. *Let $\psi \in \mathcal{H}_{phys}^{\otimes N_x N_y}$ as above. Let*

$$S = \left\{ \left(\begin{array}{c} \boxed{\begin{array}{c} \boxed{\begin{array}{cc} \uparrow & \uparrow \\ \rightarrow A \rightarrow & \rightarrow A \rightarrow \\ \uparrow & \uparrow \\ \rightarrow A \rightarrow & \rightarrow A \rightarrow \\ \uparrow & \uparrow \end{array}} \\ X \end{array} \right) \mid \begin{array}{l} \in \mathcal{H}_{phys}^{\otimes 4} \\ X \in \mathcal{H}_{virt}^{\otimes 4} \otimes \mathcal{H}_{virt}^*{}^{\otimes 4} \end{array} \right\}$$

and let $P : \mathcal{H}_{phys}^{\otimes 4} \rightarrow \mathcal{H}_{phys}^{\otimes 4}$ be the projector onto S .

Let F be a face of the $N_x N_y$ -square lattice and

$$h_F = (\text{id}_{\mathcal{H}_{phys}^{\otimes 4}} - P) \otimes \text{id}_{\mathcal{H}_{phys}^{\otimes N_x N_y - 4}}$$

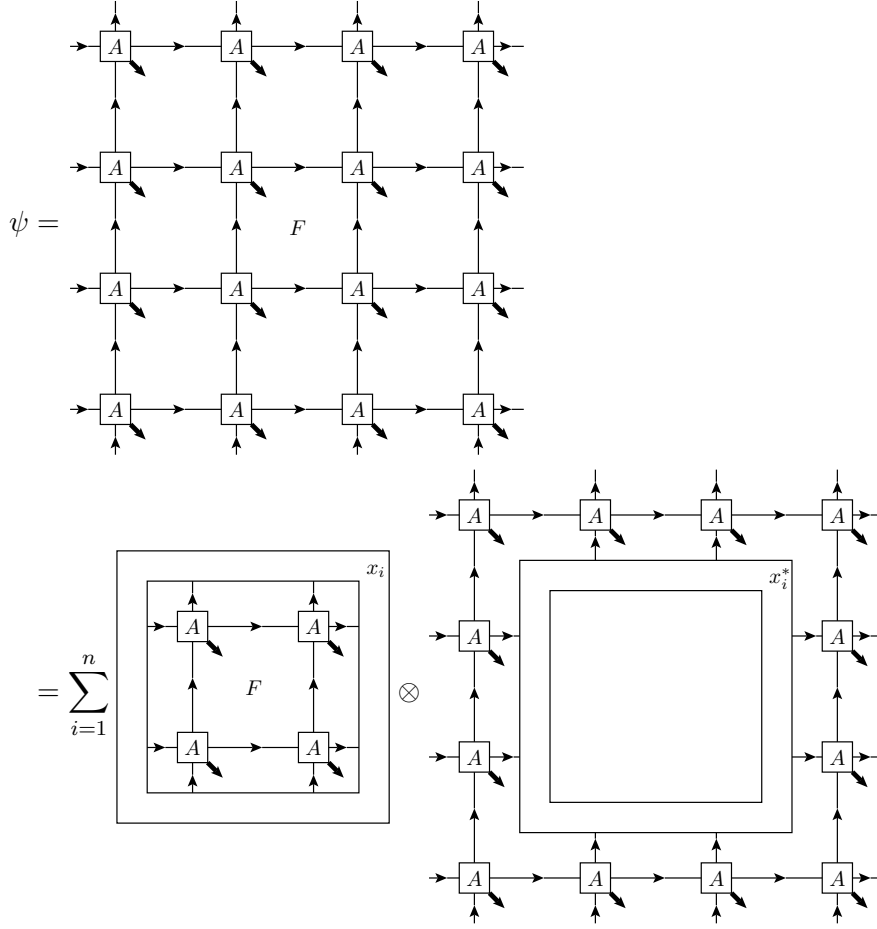
but with the factors in the tensor product reordered in such a way that h_F acts trivially on all but the four vertices at F .

Then h_F is positive semidefinite and

$$h_F \psi = 0$$

Proof. $\text{id}_{\mathcal{H}_{phys}^{\otimes 4}} - P$ is clearly positive semidefinite, so h_F is positive semidefinite. To see that ψ is a ground state of h_F , choose a basis x_1, \dots, x_n of $\mathcal{H}_{virt}^{\otimes 4} \otimes \mathcal{H}_{virt}^*{}^{\otimes 4}$ and use Lemma

2.11 to get



Because

$$(\text{id}_{\mathcal{H}_{phys}^{\otimes 4}} - P) \left[\text{2x2 grid of } A \text{ tensors with central face } F \text{ in box } x_i \right] = 0$$

for all i , it follows $h_F \psi = 0$. □

Corollary 2.13 (Parent Hamiltonian). *Let $H = \sum_F h_F$ where F runs over all faces of the N_x, N_y -square lattice. Then ψ is a ground state of H . We call H the parent hamiltonian.*

Proof. As all h_F are positive semidefinite, H is positive definite, so the eigenvalues of H are nonnegative. Because $H\psi = 0$, ψ is a ground state of H . □

Remark 2.14. Theorem 2.12 also holds if we replace the tensor network in the definition of S by the tensor network given by an arbitrary subgraph (In Theorem 2.12 the subgraph is that given by the four vertices of a face of the square lattice). The Theorem is also not specific to the N_x, N_y -square lattice, but holds on any graph.

Now that we have found a parent Hamiltonian H we turn to the questions whether H has any ground states other than ψ , i.e. whether the ground space is degenerated.

This oftentimes tells us much about the physics of the system, as we will see in section 4.4. If the tensor A that makes up the tensor network has a certain property called G -injectivity, where G is a group (not a graph!), we can give a partial answer this question, as given in [13].

Definition 2.15 (G -Invariance). Let $A \in \mathcal{H}_{virt}^{\otimes 2} \otimes \mathcal{H}_{virt}^{*\otimes 2} \otimes \mathcal{H}_{phys}$. If there is a group G with an unitary representation $(U_g)_{g \in G}$ in the virtual space, that is $U_g : \mathcal{H}_{virt} \rightarrow \mathcal{H}_{virt}$, such that for all $g \in G$

then A is called G -invariant.

Remark 2.16. All statements discussed in this thesis about G -invariant tensors will also hold if the tensor is only almost G -invariant, by which we mean that

for some constants $\alpha_g \neq 0$.

Given a closed path γ on the dual graph of the N_x, N_y -square lattice and a G -invariant tensor A we can define a state very similar to ψ : Take an element $g \in G$. Consider the tensor network given in Figure 3, but put a multiplication with U_g or with U_g^\dagger on every edge that intersects γ from left to right or from right to left respectively. An example of such a state is shown in Figure 4 (a). Let us denote such a state by $\psi_{\gamma,g}$. We have $\psi = \psi_{\gamma,e}$ for any path γ and the neutral element e of G .

Theorem 2.17 ($\psi_{\gamma,g}$ is invariant under homotopy). *Let γ_1 and γ_2 be two closed path on the dual graph of the N_x, N_y -square lattice with the same winding numbers, and let $g \in G$. Then $\psi_{\gamma_1,g} = \psi_{\gamma_2,g}$.*

The idea of the proof is shown in Figure 4. We can move the path in Figure 4(a) to the path in Figure 4(b) by inserting equation (1) on the vertex second from the top and second from the left.

Proof. We choose two paths $\tilde{\gamma}_1$ and $\tilde{\gamma}_2$ on the torus like in the definition of the winding number (Definition 2.7). Because $\tilde{\gamma}_1$ and $\tilde{\gamma}_2$ have the same winding number, differential geometry tells us that there must be a homotopy $\tilde{\delta}_t$ with $t \in [0, 1]$ and $\tilde{\delta}_0 = \tilde{\gamma}_1$ and $\tilde{\delta}_1 = \tilde{\gamma}_2$ between them. Without loss of generality at most one vertex of the N_x, N_y -square lattice lies on $\tilde{\delta}_t$ for each t . If two vertices should lie on $\tilde{\delta}_t$ for some t we can perturb the homotopy a little so that it first crosses the first vertex and the second vertex at a larger t .

Again the previous discussion is not limited to the N_x, N_y -square lattice, but holds for general lattices.

Now we have some idea how some of the ground states look like. However, we don't know whether the $\{\psi_{\gamma,g,\delta,h} | g, h \in G, gh = hg\}$ are linearly independent. Nor do we know whether there are other ground states that can't be written in this form. We will study the second question for a specific tensor in section 4.

2.4 Correlation Length

Besides the ground state degeneracy, the correlation length of a ground state oftentimes tells us interesting things about the system. In particular we can determine when the system undergoes a phase transition by looking for divergences in the correlation length. In this subsection we give a useful method to calculate the correlation length, mainly following the review [9].

Let ψ be the PEPS from Figure 3. Given a hermitian operator $O : \mathcal{H}_{phys} \rightarrow \mathcal{H}_{phys}$ let $O_{x,y} = I_{\mathcal{H}_{phys}}^{\otimes N_x N_y - 1} \otimes O$ with the factors in the tensor product reordered such that $O_{x,y}$ acts nontrivially only on the the degree of freedom at (x, y) . Then we are interested in the quantities of the type $\langle \psi, O_{x,y} O_{x+L,y} \psi \rangle / \langle \psi, \psi \rangle$ to measure the correlation between O at (x, y) and O at $(x + L, y)$. Taking scalar products is easy in tensor network notation: to calculate $\langle \phi, \psi \rangle$ for PEPS ϕ and ψ we just have to evaluate the value of the tensor network we get by connecting the tensor network that yields ψ , and the tensor network that yields ϕ with complex conjugate tensor entries along the physical vector spaces.

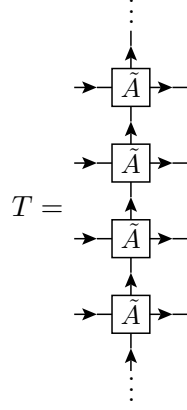
In detail, let

where the top tensor is given by A and the bottom tensor by the complex conjugate \bar{A} . Let further

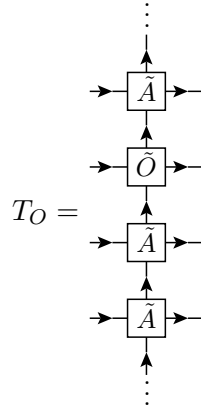
Then

$$\langle \psi, O_{x,y} O_{x+L,y} \psi \rangle =$$

where the \tilde{O} tensors are located at (x, y) and $(x + L, y)$. Define the *transfer operator*



and the similar operator



Note that T and T_O depend on N_y . Now we see

$$\langle \psi, \psi \rangle = \text{tr}(T^{N_x})$$

and

$$\langle \psi, O_{x,y} O_{x+L,y} \psi \rangle = \text{tr}(T^{N_x-L-1} T_O T^{L-1} T_O)$$

Suppose T is diagonalizable. As the set of diagonalizable operators are dense in the space of all operators, all following results by continuity also hold for non-diagonalizable T . Let $T = \sum_i \lambda_i u_i v_i^\dagger$ be the eigendecomposition of T with the right eigenvectors u_i and the left eigenvalues v_i such that $v_i^\dagger u_j = \delta_{ij}$. Then we obtain

$$\langle \psi, \psi \rangle = \sum_i \lambda_i^{N_x}$$

and

$$\langle \psi, O_{x,y} O_{x+L,y} \psi \rangle = \sum_{i,j} \lambda_i^{N_x-L-1} \lambda_j^{L-1} \langle v_i, T_O u_j \rangle \langle v_j, T_O u_i \rangle$$

Now let λ be the largest eigenvalue and $\Lambda = \{i | \lambda_i = \lambda\}$. Then as $N_x \rightarrow \infty$ only the terms with $i \in \Lambda$ contribute significantly. Hence $\langle \psi, \psi \rangle = |\Lambda| \lambda^{N_x}$ and

$$\langle \psi, O_{x,y} O_{x+L,y} \psi \rangle = \lambda^{N_x-L-1} \sum_{i \in \Lambda} \sum_j \lambda_j^{L-1} \langle v_i, T_O u_j \rangle \langle v_j, T_O u_i \rangle$$

So we get

$$\frac{\langle \psi, O_{x,y} O_{x+L,y} \psi \rangle}{\langle \psi, \psi \rangle} = |\Lambda|^{-1} \lambda^{-2} \sum_{i \in \Lambda} \sum_j \left(\frac{\lambda_j}{\lambda} \right)^{L-1} \langle v_i, T_O u_j \rangle \langle v_j, T_O u_i \rangle = C_1 + C_2 \exp(-L/\xi)$$

where the second equality holds in the limit of large L and for constants C_1 and C_2 and the correlation length $\xi = (\log(\lambda/\lambda'))^{-1}$, where λ' is the second largest eigenvalue of T .

So we see that we can calculate the correlation length from the first two eigenvalues of the transfer operator. Note that when we want to consider infinite systems with $N_y \rightarrow \infty$ we need to take λ' to be the largest eigenvalue that is even in the limit $N_y \rightarrow \infty$ not equal to λ .

3 Quantum N -mer Models

In the following section we will define quantum N -mer models and show how to write them as tensor networks in section 3.1. We characterize the ground space of the parent Hamiltonians of quantum N -mer models in section 3.2 and show how to distinguish different ground states using topological invariants in section 3.3.

3.1 Quantum N -mer Models as Tensor Networks

Quantum dimer models have first been introduced by Rokhsar and Kivelson [2] to study high-temperature superconductors. Since then it was realized that the quantum dimer model possess many striking features, like topological order, which we will explore section 4.4, and unusual types of excitations. A good review of quantum dimer models not using tensor network notation is given in [14]. Quantum trimer models, which are a natural generalization of quantum dimer models, have been introduced and studied on the square lattice using tensor network methods by [6]. In this section we will define a general quantum N -mer model, see how we can write it as a tensor network and study its parent Hamiltonian.

Let us first consider a classical model. Given some lattice as a graph G we can select some edges of G such that each vertex is in exactly one of those edges. In graph theory this is known as a perfect matching, we will call it a dimer covering. The generalization to N -mer coverings is straight forward: We want to select $N - 1$ -tuples of edges of G that form a non intersecting string, i.e. the first and second edge share a vertex, the second and third edge share a vertex, etc. Formally we can define this as a N -perfect matching:

Definition 3.1 (N -perfect matching). Let G be a graph with vertices V and edges E . A directed perfect N -mer matching is a set $P \subseteq E^{N-1}$ such that

1. for each $(e_1, \dots, e_{N-1}) \in P$ there are pairwise distinct $v_0, \dots, v_{N-1} \in V$ such that e_i connects v_{i-1} and v_i for $i = 1, \dots, N - 1$ and
2. for each $v \in V$ there is exactly one element $(e_1, \dots, e_{N-1}) \in P$ and at least one $i \in \{1, \dots, N - 1\}$ such that e_i is connected to v .

The elements of P are called N -mers. We can define an equivalence relation \sim between to directed perfect matchings as $P \sim Q$ if and only if for each $(e_1, \dots, e_{N-1}) \in P$ either $(e_1, \dots, e_{N-1}) \in Q$ or $(e_{N-1}, \dots, e_1) \in Q$. An equivalence class $[P]$ is called an N -perfect matching.

Remark 3.2.

1. \sim is clearly reflexive and transitive. From property 2 of the definition it follows that P and Q contain the same number of N -mers, namely $|V|/N$. So if $P \sim Q$ and $(e_1, \dots, e_N) \in Q$, then either $(e_1, \dots, e_N) \in P$ or $(e_N, \dots, e_1) \in P$, so $Q \sim P$. Hence \sim is a proper equivalence relation.
2. Directed graphs are of course also graphs. We want to stress that for a N -perfect matching of a directed graph the direction of the edges in property 1 is irrelevant.

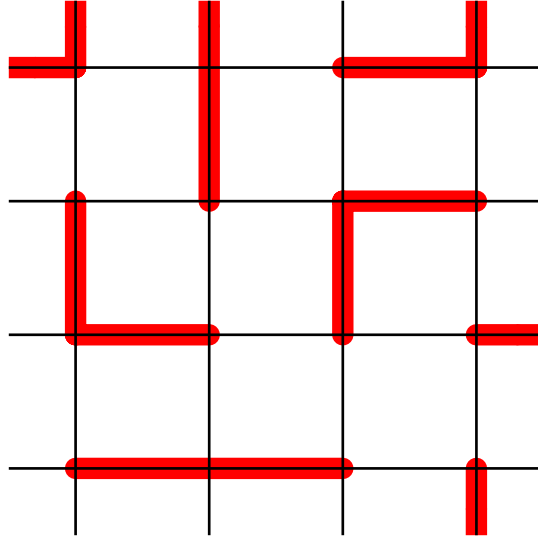


Figure 5: An example of a 3-perfect matching on a part of a square lattice

An example of a 3-perfect matching, or trimer covering, is shown in Figure 5.

While N -perfect matchings might be the most natural way to describe a N -mer covering, we need a different description more suited to the language of tensor networks. This description we want to call a constraint model:

- Definition 3.3.**
1. Let $G = (V, E)$ be a graph, and let M be a finite set. Let for each vertex $v \in V$ E_v be the set of edges connected at v . If $\mathcal{M}_v \subseteq \{\omega_v : E_v \rightarrow M\}$ is a subset of all functions from the edges at v to M , then the family $(\mathcal{M}_v)_{v \in V}$ is called a constraint model.
 2. A family $(\omega_v)_{v \in V}$ of maps such that $\omega_v \in \mathcal{M}_v$ and such that for each edge e connecting vertices v_1 and v_2 it holds that $\omega_{v_1}(e) = \omega_{v_2}(e)$ is called a vertex configuration in the constraint model $(\mathcal{M}_v)_{v \in V}$. The corresponding function $\omega : E \rightarrow M$ given by $\omega(e) = \omega_v(e)$ where v is any vertex attached to e is called an edge configuration in the constraint model.

As an example of a constraint model consider a directed graph G with vertices V and edges E . Define $\sigma : V \times E \rightarrow \{-1, 1\}$ as $\sigma(v, e) = 1$ if e ends in v and $\sigma(v, e) = -1$ if e starts in v . Let $N \in \mathbb{N}$ and choose $M = \mathbb{Z}_N$. Set

$$\mathcal{M}_v = \left\{ e \mapsto \begin{cases} \sigma(v, e)n & \text{if } e = e_1 \\ -\sigma(v, e)(n+1) & \text{if } e = e_2 \\ 0 & \text{otherwise} \end{cases} \middle| e_1, e_2 \in E_v, e_1 \neq e_2, n \in \mathbb{Z}_N \right\} \quad (3)$$

We will call this the N -mer constraint model. All elements $\omega_v \in \mathcal{M}_v$ for a trimer constraint model on a vertex of the square lattice are shown in Figure 6. The number shown at each edge e is the value $\omega_v(e)$. It is easy to verify that placing one of the ω_v at each vertex such that the common edges match leads to a trimer covering, where the trimers are given by the edges with $\omega_v(e) \neq 0$. Also, each trimer covering can be written in such a form. The constraint model obtained is identical to that in [6]. The next theorem shows why N -perfect matchings can always be described by the N -mer constraint model for a general graph and arbitrary N .

Theorem 3.4 (Bijection between N -perfect matchings and N -mer constraint model).
For any graph G and $N \in \mathbb{N}$ there is a bijection \mathcal{F} between N -perfect matchings of G and

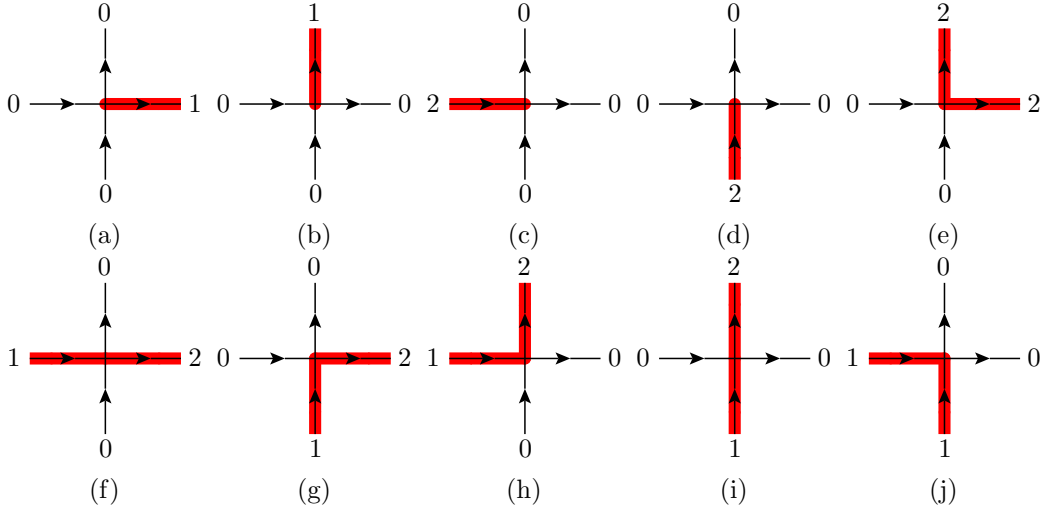


Figure 6: All allowed configurations for a trimer constraint model on a square lattice. The numbers on an edge e show $\omega_v(e)$. The edges with $\omega_v(e) \neq 0$ make up the trimers.

vertex configurations in the N -mer constraint model with the following property: For $[P]$ and $[Q]$ two perfect matchings, let v be a vertex in one of the N -mers in $P \cap Q$. Then $\mathcal{F}(P)_v = \mathcal{F}(Q)_v$.

We will call this property *locality*, because it says that when we change a perfect matching only in the vicinity of some vertex, the corresponding vertex configuration also only changes in the vicinity of this vertex.

The idea of the proof is to assign to an edge e in an N -mer the number of edges of the N -mer which lie on the side of e on which e starts (including e itself). So for example the first/last edge of an N -mer will be assigned 1 if the edge is directed to the inside of the N -mer, and $N - 1$ if the edge is directed to the end of the N -mer.

Proof. Let $[P]$ be a N -perfect matching and $(e_1, \dots, e_{N-1}) \in P$. Let v_0, \dots, v_{N-1} be the vertices such that e_i connects v_{i-1} and v_i for $i = 1, \dots, N - 1$. For $n = 0, \dots, N - 1$ set if $n \neq 0$

$$\mathcal{F}(P)_{v_n}(e_n) = \sigma(v_n, e_n)n$$

if $n \neq N - 1$

$$\mathcal{F}(P)_{v_n}(e_{n+1}) = -\sigma(v_n, e_{n+1})(n + 1)$$

and for all edges e except e_n or e_{n+1} that are connected to v_n

$$\mathcal{F}(P)_{v_n}(e) = 0$$

Because of property 2 in Definition 3.1 this completely defines $\mathcal{F}(P)$. From this definition of \mathcal{F} it is immediately clear that $\mathcal{F}(P)_v \in \mathcal{M}_v$ for all vertices v .

To check that \mathcal{F} is well defined we still need to check that $\mathcal{F}(P) = \mathcal{F}(Q)$ if $P \sim Q$. To see this, let Q be a directed N -perfect matching with $P \sim Q$. If $(e_1, \dots, e_{N-1}) \in Q$, then clearly $\mathcal{F}(P)_{v_n} = \mathcal{F}(Q)_{v_n}$ for $n = 0, \dots, N - 1$. If instead $(e_{N-1}, \dots, e_1) \in Q$ denote $f_n = e_{N-n}$ and $w_n = v_{N-n-1}$, so that $(e_{N-1}, \dots, e_1) = (f_1, \dots, f_{N-1})$ and $(v_{N-1}, \dots, v_0) = (w_0, \dots, w_{N-1})$. Then we see

$$\begin{aligned} \mathcal{F}(Q)_{v_n}(e_n) &= \mathcal{F}(Q)_{w_{N-n-1}}(f_{N-n}) = -\sigma(w_{N-n-1}, f_{N-n})(N - n) \\ &= \sigma(w_{N-n-1}, f_{N-n})n = \sigma(v_n, e_n)n = \mathcal{F}(P)_{v_n}(e_n) \end{aligned}$$

and

$$\begin{aligned}\mathcal{F}(Q)_{v_n}(e_{n+1}) &= \mathcal{F}(Q)_{w_{N-n-1}}(f_{N-n-1}) = \sigma(w_{N-n-1}, f_{N-n-1})(N-n-1) \\ &= -\sigma(w_{N-n-1}, f_{N-n-1})(n+1) = -\sigma(v_n, e_{n+1})(n+1) = \mathcal{F}(P)_{v_n}(e_{n+1})\end{aligned}$$

Now we still have to check that $\mathcal{F}(P)$ is indeed a vertex configuration. To see this, note that for $n = 1, \dots, N-1$

$$\mathcal{F}(P)_{v_{n-1}}(e_n) = -\sigma(v_{n-1}, e_n)n = \sigma(v_n, e_n)n = \mathcal{F}(P)_{v_n}(e_n)$$

where we used the fact that e_n connects v_{n-1} and v_n , so $\sigma(v_n, e_n) = -\sigma(v_{n-1}, e_n)$. This shows that $\mathcal{F}(P)_v$ is consistent on all edges that are in one of the N -mers in P . But for all other edges e , $\mathcal{F}(P)_v(e) = 0$ for both vertices v on that edge. So $\mathcal{F}(P)$ is indeed a vertex configuration.

Now we prove that \mathcal{F} is injective: Suppose $\mathcal{F}(P) = \mathcal{F}(Q) =: (\omega_v)_v$. Let ω be the corresponding edge configuration. Because $\omega(e) \neq 0$ if and only if e is in one of the N -mers in P , the edges e with $\omega(e) \neq 0$ form strings of length $N-1$. So we see that because the set of edges that are mapped to 0 by $\mathcal{F}(P)$ and $\mathcal{F}(Q)$ agree, it must be $P \sim Q$.

For bijectivity we still have to show surjectivity: Let $(\omega_v)_v$ be a vertex configuration and ω the corresponding edge configuration. Let e be an edge with $\omega(e) \neq 0$. Set $m = \omega(e)$, $e_m = e$ and v_m the end of e . Then $\sigma(v_m, e_m) = 1$, so $\sigma(v_m, e_m)\omega_{v_m}(e_m) = m$. Now e_m is either e_1 or e_2 in equation (3). If e_m is e_1 , then $n = m$, if e_m is e_2 , then $n = -(m+1)$, where n is the n from (3). In either case, there is a unique other edge, which we will call e_{m+1} with $\sigma(v_m, e_{m+1})\omega_{v_m}(e_{m+1}) = -(m+1)$. e_{m+1} is connected to v_m and another vertex, which we will call v_{m+1} . Then $\sigma(v_{m+1}, e_{m+1})\omega_{v_{m+1}}(e_{m+1}) = (m+1)$. By repeating this argument as long as $m \leq N-1$, we can find edges $e_m, e_{m+1}, \dots, e_{N-1}$ and vertices v_m, \dots, v_{N-1} with $\sigma(v_k, e_k)\omega_{v_k}(e_k) = k$ for $k = m, \dots, N-1$.

We can do the same by decrementing m : Set v_{m-1} to be the start of e_m . Then $\sigma(v_{m-1}, e_m)\omega_{v_{m-1}}(e_m) = -m$. By repeating the argument from above, we can find an edge e_{m-1} that is connected to v_{m-1} with $\sigma(v_{m-1}, e_{m-1})\omega_{v_{m-1}}(e_{m-1}) = (m-1)$. Again repeating this argument as long as $m > 0$ we can find vertices v_0, \dots, v_{m-1} and edges e_1, \dots, e_{m-1} with $\sigma(v_k, e_k)\omega_{v_k}(e_k) = k$.

Constructing all of those N -mers (e_1, \dots, e_{N-1}) gives an N -perfect matching P . This matching satisfies

$$\mathcal{F}(P)_{v_n}(e_n) = \sigma(v_n, e_n)n = \omega_{v_n}(e_n)$$

and

$$\mathcal{F}(P)_{v_n}(e_{n+1}) = -\sigma(v_n, e_{n+1})(n+1) = \sigma(v_{n+1}, e_{n+1})(n+1) = \omega_{v_{n+1}}(e_{n+1}) = \omega_{v_n}(e_{n+1})$$

where we have used that $\sigma(v_n, e_n)^2 = 1$. So \mathcal{F} is surjective.

The locality property follows immediately from the definition of \mathcal{F} , because $\mathcal{F}(P)_v$ only depends on the N -mer in P that contains an edge connected to v . \square

For a constraint model $(\mathcal{M}_v)_v$ on a graph G we can consider the corresponding quantum state given by the equal superposition of all vertex configurations in this constraint model. This state is an element of $\bigotimes_{v \in V} \mathcal{H}_{phys}^{(v)}$, where $\mathcal{H}_{phys}^{(v)}$ is the free vector space of \mathcal{M}_v over \mathbb{C} , i.e. a vector space in which the elements of \mathcal{M}_v form a basis. We equip

$\mathcal{H}_{phys}^{(v)}$ with the inner product for which the elements of \mathcal{M}_v are orthonormal. Then we want to consider the quantum state

$$\sum_{(\omega_v)_v} \bigotimes_{v \in V} \omega_v$$

where we sum over all vertex configurations $(\omega_v)_v$ in the constraint model. If the constraint model is the N -mer constraint model, we will call this state the quantum N -mer state. This state can be written as a tensor network: Choose \mathcal{H}_{virt} to be the free vector space of M over \mathbb{C} (or \mathbb{R} , for our considerations this is irrelevant). If we denote by $E_v^{(s)}$ the edges starting in v , and by $E_v^{(e)}$ the edges ending in v , we can define the tensor

$$A_v = \sum_{\omega_v \in \mathcal{M}_v} \omega_v \otimes \bigotimes_{e \in E_v^{(s)}} \omega_v(e) \otimes \bigotimes_{e \in E_v^{(e)}} \omega_v(e)^* \in \mathcal{H}_{phys}^{(v)} \otimes \mathcal{H}_{virt}^{\otimes |E_v^{(s)}|} \otimes \mathcal{H}_{virt}^* \otimes |E_v^{(e)}|$$

The tensor network we get by placing A_v on the vertex v for all vertices yields the above quantum state.

3.2 Ground States of Constraint Models

Now we turn to the question what ground states the Hamiltonian h_F given in Theorem 2.12 has, if the tensor network is described by a constraint model. We will see that the ground states are exactly those states which at least on F look like a vertex configuration and have equal amplitude for configurations which only differ on the vertices of F .

Theorem 3.5. *Let \mathcal{M}_v be a constraint model on the N_x, N_y -square lattice, let V be the vertices of that lattice. Let F be a face, and let V' be the vertices at that face, E' the edges that connect two vertices in V' , and B the edges that connect a vertex in V' with a vertex in $V \setminus V'$. Then*

$$\psi = \sum_{(\omega_v \in \mathcal{M}_v)_{v \in V}} \psi_{(\omega_v)_v} \bigotimes_{v \in V} \omega_v$$

is a ground state of h_F if and only if

1. $\psi_{(\omega_v)_v} = 0$ if not for all $e \in E'$ and vertices v_1 and v_2 connected by e it is $\omega_{v_1}(e) = \omega_{v_2}(e)$ and
2. $\psi_{(\omega_v)_v} = \psi_{(\eta_v)_v}$ if $\omega_v = \eta_v$ for $v \in V \setminus V'$ and $\omega_v(e) = \eta_v(e)$ for all $e \in B$ and v the vertex of e in V' .

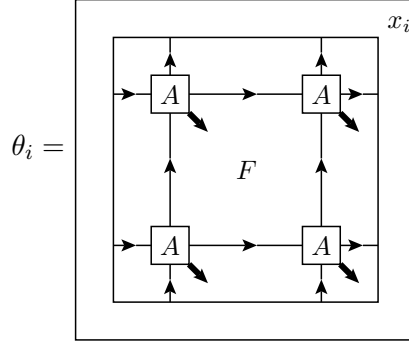
Proof. For the first direction, suppose that $h_F \psi = 0$. Let ϕ_1, \dots, ϕ_n ($n \in \mathbb{N}$) be an orthogonal basis of $\bigotimes_{v \in V \setminus V'} \mathcal{H}_{phys}^{(v)}$. Then there are $\theta_1, \dots, \theta_n \in \bigotimes_{v \in V} \mathcal{H}_{phys}^{(v)}$ such that

$$\psi = \sum_{i=1}^n \theta_i \otimes \phi_i$$

Because $h_F \psi = 0$ and the ϕ_i are orthogonal, there is an $x_i \in \mathcal{B}$ with

$$\mathcal{B} = \bigotimes_{e \in B} \begin{cases} \mathcal{H}_{virt} & \text{if } e \text{ ending in } F \\ \mathcal{H}_{virt}^* & \text{if } e \text{ starting in } F \end{cases}$$

such that



Let for $m \in M^B$

$$b_m = \bigotimes_{e \in B} \begin{cases} m_e & \text{if } e \text{ ending in } F \\ m_e^* & \text{if } e \text{ starting in } F \end{cases}$$

Then the b_m form a basis of \mathcal{B} . By expanding x_i for each i in this basis we see that there are $\alpha_m \in \bigotimes_{v \in V \setminus V'} \mathcal{H}_{phys}^{(v)}$ for m in $m \in M^B$ such that

$$\psi = \sum_{m \in M^B} \begin{array}{|c|} \hline \begin{array}{|c|} \hline \begin{array}{ccc} \rightarrow & & \rightarrow \\ \hline \boxed{A} & & \boxed{A} \\ \hline \rightarrow & & \rightarrow \\ \hline \uparrow & & \uparrow \\ \hline \boxed{A} & & \boxed{A} \\ \hline \rightarrow & & \rightarrow \\ \hline \uparrow & & \uparrow \\ \hline \end{array} \\ \hline \end{array} \otimes \alpha_m$$

F

Now we see that

$$\begin{array}{|c|} \hline \begin{array}{|c|} \hline \begin{array}{ccc} \rightarrow & & \rightarrow \\ \hline \boxed{A} & & \boxed{A} \\ \hline \rightarrow & & \rightarrow \\ \hline \uparrow & & \uparrow \\ \hline \boxed{A} & & \boxed{A} \\ \hline \rightarrow & & \rightarrow \\ \hline \uparrow & & \uparrow \\ \hline \end{array} \\ \hline \end{array} \otimes \omega_{v'} \\ \hline \end{array} = \sum_{(\omega_v)_{v \in V'} \in X_m} \bigotimes_{v \in V'} \omega_v$$

F

where X_m is the set of all $(\omega_v)_{v \in V'}$ with $\omega_v \in \mathcal{M}_v$ for which property 1 holds and for which for all $e \in B$ with the vertex v in V' it is $\omega_v(e) = m_e$. Hence, ψ must have property 1, and for $(\omega_v)_v$ and $(\eta_v)_v$ as in property 2 we see that for $m \in M^B$, $m_e := \eta_v(e) = \omega_v(e)$ it holds that

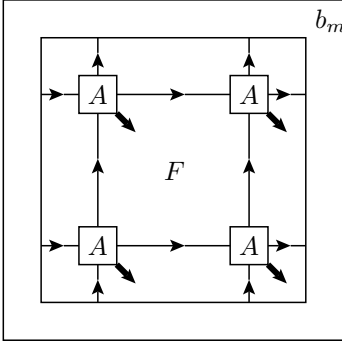
$$\langle \bigotimes_{v \in V} \omega_v, \psi \rangle = \langle \bigotimes_{v \in V \setminus V'} \omega_v, \alpha_m \rangle = \langle \bigotimes_{v \in V \setminus V'} \eta_v, \alpha_m \rangle = \langle \bigotimes_{v \in V} \eta_v, \psi \rangle$$

so property 2 holds for ψ .

To see the other direction, suppose ψ satisfies properties 1 and 2. Then because of property 1, ψ can be written as

$$\psi = \sum_{(\omega_v \in \mathcal{M}_v)_{v \in V \setminus V'}} \sum_{m \in M^B} \sum_{(\omega'_v)_{v \in V'} \in X_m} \psi_{(\omega'_v)_{v \in V'}} \bigotimes_{v \in V'} \omega'_v \otimes \bigotimes_{v \in V \setminus V'} \omega_v$$

But by property 2, $\psi_{(\omega_v)_{v \in V}}$ only depends on $(\omega_v)_{v \in V \setminus V'}$ and on m , so there are $c_{(\omega_v)_{v \in V \setminus V'}, m}$ such that

$$\begin{aligned} \psi &= \sum_{(\omega_v \in \mathcal{M}_v)_{v \in V \setminus V'}} \sum_{m \in M^B} c_{(\omega_v)_{v \in V \setminus V'}, m} \left(\sum_{(\omega'_v)_{v \in V'} \in X_m} \bigotimes_{v \in V'} \omega'_v \right) \bigotimes_{v \in V \setminus V'} \omega_v \\ &= \sum_{(\omega_v \in \mathcal{M}_v)_{v \in V \setminus V'}} \sum_{m \in M^B} c_{(\omega_v)_{v \in V \setminus V'}, m} \left(\text{Diagram} \right) \bigotimes_{v \in V \setminus V'} \omega_v \end{aligned}$$


So we see that $h_F \psi = 0$. □

Corollary 3.6 (Ground States of Quantum N -mer Models). *The ground states of the parent hamiltonian $H = \sum_F h_F$ are given by*

$$\sum_{(\omega_v)_v} \psi_{(\omega_v)_v} \bigotimes_{v \in V} \omega_v$$

where we sum over all vertex configurations $(\omega_v)_v$, with $\psi_{(\omega_v)_v} = \psi_{(\eta_v)_v}$ whenever there are vertex configurations $(\rho_{0v})_v, \dots, (\rho_{nv})_v$ for an $n \in \mathbb{N}$ such that $(\omega_v)_v = (\rho_{0v})_v$, $(\eta_v)_v = (\rho_{nv})_v$, and for $i = 0, \dots, n-1$ $(\rho_{iv})_v$ and $(\rho_{i+1v})_v$ differ only at the vertices at a single face of the lattice.

Proof. Because each edge is in some face of the lattice, property 1 of Theorem 3.5 must hold for all edges, so any ground state must be a superposition of vertex configurations. Because $H\psi = 0$ if and only if $h_F\psi = 0$ for all F , any two vertex configurations which only differ on a face must have equal amplitude. Hence, all ground states must be in the form given in the corollary. Also any state in the above form must be a ground state of h_F for all F , because any two vertex configurations that only differ on F have equal amplitude. □

Remark 3.7. Again, the result is not limited to the Nx, Ny -square lattice, but holds for any graph G . We can also replace the single face by any subgraph G' . Then the ground states of $h_{G'}$ are given by all superpositions of vertex configuration with equal amplitude whenever two vertex configurations only differ on G' . The proof in this general setting works just like the proof for Theorem 3.5.

Applying Corollary 3.6 to the dimer constraint model gives the same Hamiltonian as originally given in [2]. Applying it for the trimer constraint model on the subgraphs given by 3×3 -square of vertices (as opposed to the 2×2 squares of vertices on a single face), gives the trimer Hamiltonian given in [6].

Now for a given lattice we want to understand which is the minimal number of ground states for hamiltonians $H = \sum_{G'} h_{G'}$, where we can choose any subgraphs that are a lot smaller than the size of the lattice. This is equivalent to asking which vertex configuration can be transformed to which other vertex configuration by a chain on changes which each only change the vertex configuration on one of the subgraphs G' . We will call such a single change a *local move* of size d , where d is the number of full edges of G' .

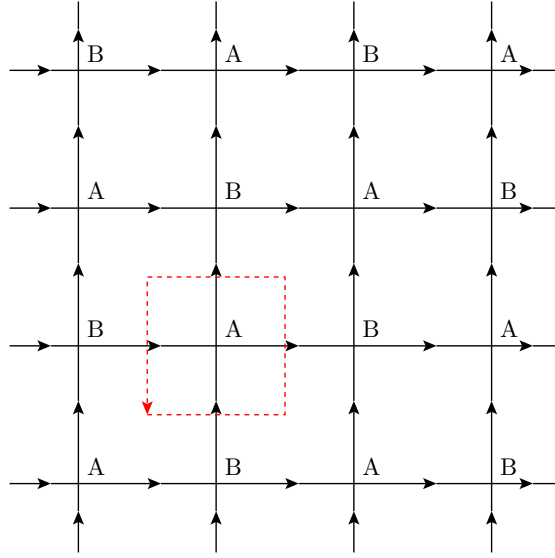


Figure 7: Grouping of the vertices in the sets A and B . The dashed line shows the path ϵ encircling a vertex counterclockwise.

3.3 Topological Invariants

For the N -mer constraint model in equation (3) we notice that for each $\omega_v \in \mathcal{M}_v$ it holds that $\sum_e -\sigma(v, e)\omega_v(e) = 1$, where we sum over all edges e at the vertex v . Using this, we see that the corresponding tensor is almost \mathbb{Z}_N invariant in the sense of Remark 2.16, where we choose the representation

$$U_k = \text{diag}(1, e^{2\pi i k/N}, e^{2\pi i 2k/N}, \dots, e^{2\pi i (N-1)k/N})$$

Here, putting a multiplication with U_k or U_k^\dagger on each edge of the tensor A changes it only by a multiplication with $\alpha_k = e^{2\pi i k/N}$. So we already now how to construct some of the ground states by the method given in Theorem 2.18. We can find the analogous statement in terms of local moves. For this, we first need the notion of an integral of a function from the edges of the lattice to some abelian group G :

Definition 3.8 (Integral along a Path). Let G be an abelian group and $\omega : E \mapsto G$ a map from the edges of a lattice to G . Let $\gamma = (F_0, \dots, F_n)$ be a path on the dual lattice, and e_1, \dots, e_n the edges such that e_i is between the faces F_{i-1} and F_i for $i = 1, \dots, n$. We define

$$\int_\gamma \omega = \sum_{i=1}^n \begin{cases} \omega(e_i) & \text{if } e_i \text{ crosses } \gamma \text{ from left to right} \\ -\omega(e_i) & \text{if } e_i \text{ crosses } \gamma \text{ from right to left} \end{cases}$$

to be the integral of ω along the path γ .

Now for any vertex configuration of the N -mer constraint model $(\omega_v)_v$ and the corresponding edge configuration ω , and any vertex v and γ the path that encircles v counterclockwise, it is $\int_\gamma \omega = -1$. We can use this in a theorem similar to Theorem 2.17. The path ϵ is shown in Figure 7.

Theorem 3.9 (Local moves do not change integrals along closed paths). Let $(\mathcal{M}_v)_v$ be a constraint model with values in M . Let $f : E \times M \rightarrow G$ be a map, where E is the set of edges of the lattice and G is a commutative group. Let for an edge configuration ω denote with $\tilde{\omega} : E \rightarrow G$ the map given by $e \mapsto f(e, \omega(e))$. Suppose that for any vertex v there is a $\rho_v \in G$ such that for all edge configurations ω

$$\int_\epsilon \tilde{\omega} = \rho_v$$

where ϵ is the path that encircles v counterclockwise. Then for any closed path γ and edge configurations ω and η that differ by a local move

$$\int_{\gamma} \tilde{\omega} = \int_{\gamma} \tilde{\eta}$$

Proof. Because ω and η that only differ by a local move there is a path γ' with the same winding numbers as γ that only crosses edges on which ω and η are identical. Then we can find paths $\delta_0, \dots, \delta_n$ ($n \in \mathbb{N}$) like in Theorem 2.17, such that $\delta_0 = \gamma$, $\delta_n = \gamma'$, and for each $i \in \{1, \dots, n\}$ there is exactly one vertex v_i such that the edges at v_i which are cut by δ_{i-1} are different from those cut by δ_i . Hence, $\int_{\delta_i} \tilde{\omega} - \int_{\delta_{i-1}} \tilde{\omega} = \int_{\epsilon_{i,\pm}} \tilde{\omega}$, where $\epsilon_{i,+}$ is the path that encircles v_i counterclockwise, and $\epsilon_{i,-}$ is the path that encircles v_i clockwise. But we know that $s_i := \int_{\epsilon_{i,\pm}} \tilde{\omega} = \pm \rho_{v_i}$. Therefore,

$$\int_{\gamma'} \tilde{\omega} - \int_{\gamma} \tilde{\omega} = \sum_{i=1}^n s_i$$

By the same argument we get

$$\int_{\gamma'} \tilde{\eta} - \int_{\gamma} \tilde{\eta} = \sum_{i=1}^n s_i$$

Because ω and η agree on all edges cut by γ' , we also have

$$\int_{\gamma'} \tilde{\omega} = \int_{\gamma'} \tilde{\eta}$$

so together we get

$$\int_{\gamma} \tilde{\omega} = \int_{\gamma} \tilde{\eta}$$

□

So we see that if for a constraint model we can find such a function f , we can choose two paths γ and δ with winding numbers $(1,0)$ and $(0,1)$ and get two invariants with values in G . Let us call these invariants *loop invariants*. Two edge configurations which differ by at least one of the loop invariants can't be related by a chain of local moves, so their amplitudes in a ground state can be chosen independent of each other.

If we consider the N -mer constraint model, we get two loop invariants by just choosing $f(e, n) = n \in \mathbb{Z}_N$. However, for some N and some lattices, we can find more loop invariants: Consider the dimer constraint model on the N_x, N_y -square lattice with N_x and N_y even. Set

$$A = \{(n, m) | n, m \in \mathbb{N}, n + m \text{ is even}\} \in \mathbb{T}_{N_x, N_y}$$

and

$$B = \{(n, m) | n, m \in \mathbb{N}, n + m \text{ is odd}\} \in \mathbb{T}_{N_x, N_y}$$

Then $A \cup B$ are the vertices of the N_x, N_y -square lattice. The two sets are shown in Figure 7. Note that each edge connects a vertex from A with a vertex from B , so the N_x, N_y -square lattice is bipartite.

Now set $f : E \times \mathbb{Z}_2 \rightarrow \mathbb{Z}$ to be

$$f(e, n) = \begin{cases} n & \text{if } e \text{ starts in } A \\ -n & \text{if } e \text{ ends in } A \end{cases}$$

where we interpret n as a value in \mathbb{Z} by interpreting $0 \in \mathbb{Z}_2$ as $0 \in \mathbb{Z}$ and $1 \in \mathbb{Z}_2$ as $1 \in \mathbb{Z}$. Let $v \in A$. Because the edges connected to v that start in v are exactly those which cross the path ϵ , which encircles v counterclockwise, from left to right, we get that for any edge configuration ω

$$\int_{\epsilon} \tilde{\omega} = \sum_e \omega(e)$$

where we sum over all edges at v and we interpret $\omega(e)$ as elements in \mathbb{Z} . Noting that for the dimer model on the square lattice we have

$$\mathcal{M}_v = \left\{ e \mapsto \begin{cases} 1 & \text{if } e = e_1 \\ 0 & \text{if } e \neq e_1 \end{cases} \middle| e_1 \text{ edge connected at } v \right\}$$

we see that

$$\int_{\epsilon} \tilde{\omega} = 1$$

for all ω . If instead we consider a vertex $v \in B$, by the same argument we get

$$\int_{\epsilon} \tilde{\omega} = -1$$

for all ω . Hence we can find loop invariants with values in \mathbb{Z} .

4 The Trimer Model on the Kagome Lattice

In the previous section we have shown that two N -mer configurations with different loop invariants can't be transformed into each other using a chain of local moves. In section 4.1-4.3 we will also show the reverse statement for the trimer model on the N_x, N_y -kagome lattice: There is a D independent of N_x and N_y such that given two trimer configurations with the same two \mathbb{Z}_3 loop invariants, we can find a chain of local moves of size D to transform the one configuration into the other. The same statement for dimers on the kagome lattice was proven in [15].

We start by showing equivalence of the N -mer constraint model on the kagome lattice to a model on the honeycomb lattice in section 4.1. In sections 4.2 and 4.3 we then complete the proof. In section 4.4 we show that the trimer model on the kagome lattice does not exhibit topological order, but a similar model, which we get by changing the amplitudes in the superposition of all trimer configurations, does.

4.1 From Kagome to Honeycomb Lattice

Let us define the *honeycomb constraint model* to be the constraint model on the honeycomb lattice as

$$\mathcal{M}_v = \{\omega_v : E \rightarrow \mathbb{Z}_3 \mid \omega_v(e_1) + \omega_v(e_2) + \omega_v(e_3) = 0, \exists i : \omega(e_i) \neq 0\}$$

where e_1, e_2, e_3 are the three edges at the vertex v . Note that on the honeycomb lattice with the edges oriented like in Figure 1 either all edges connected at a vertex start in this vertex, or all edges connected at the vertex end at this vertex. Hence $\int_\epsilon \omega = 0$ for an edge configuration ω and a path ϵ encircling a vertex, so there are two loop invariants for the honeycomb constraint model. Now we can show that there is a mapping from the trimer constraint model on the kagome lattice to the honeycomb constraint model, in such a way that the loop invariants of two edge configuration on the kagome lattice agree if and only if the loop invariants of the corresponding edge configurations in the honeycomb constraint model agree.

Theorem 4.1 (Mapping from Kagome to Honeycomb Lattice). *There is a map \mathcal{F} from the vertex configurations in the trimer constraint model on the N_x, N_y -kagome lattice to the vertex configurations in the honeycomb constraint model on the N_x, N_y -honeycomb lattice such that*

1. \mathcal{F} is surjective,
2. If $\mathcal{F}(\omega) = \mathcal{F}(\eta)$ for two vertex configurations on the trimer constraint model, then there is a chain of local moves of size 3 transforming $(\omega_v)_v$ to $(\eta_v)_v$,
3. If $\mathcal{F}(\omega)$ and $\mathcal{F}(\eta)$ differ on d edges, then there is an edge configuration ω' with $\mathcal{F}(\omega) = \mathcal{F}(\omega')$ such that ω' and η differ on at most $6d$ edges, and
4. For each path γ on the dual of the kagome lattice there is a path γ' on the dual of the honeycomb lattice with the same winding numbers and such that if $\int_\gamma \omega = \int_\gamma \eta$ then $\int_{\gamma'} \mathcal{F}(\omega) = \int_{\gamma'} \mathcal{F}(\eta)$

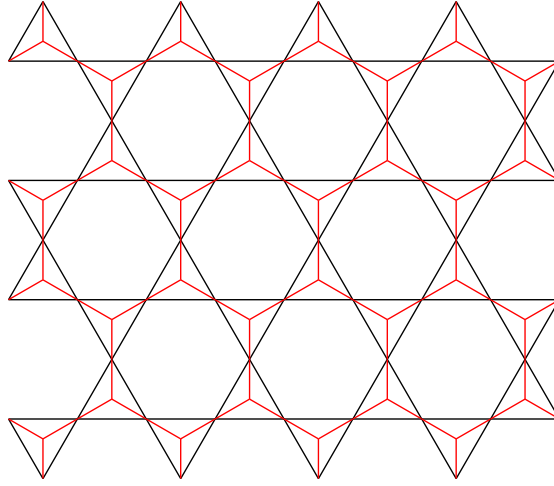


Figure 8: We can get the honeycomb lattice by viewing the triangles in the kagome lattice as vertices

Proof. We can get the honeycomb lattice from the kagome lattice by taking the triangles in the kagome lattice as vertices in the honeycomb lattice and the vertices in the kagome lattice as the edges in the honeycomb lattice. This procedure is shown in Figure 8.

Let ω be an edge configuration in the trimer constraint model, and let v be a vertex in the honeycomb lattice. We want to define $\mathcal{F}(\omega)_v$ in terms of the three edges of the triangle T around v . For this, consider the 3-perfect matching P corresponding to ω by Theorem 3.4. An edge e connected to v intersects exactly one vertex v_e of the kagome lattice. Let T' be the triangle on v_e that is not T . There is exactly one trimer $t \in P$ such that one of the edges in t is connected to v_e . If T points upward, we set

$$\mathcal{F}(\omega)_v(e) = \begin{cases} 0 & t \text{ has an edge in } T \text{ and an edge in } T' \\ 1 & t \text{ has an edge in } T \text{ and no edge in } T' \\ 2 & t \text{ has no edge in } T \text{ and an edge in } T' \end{cases}$$

If T points downwards, we set

$$\mathcal{F}(\omega)_v(e) = \begin{cases} 0 & t \text{ has an edge in } T \text{ and an edge in } T' \\ 2 & t \text{ has an edge in } T \text{ and no edge in } T' \\ 1 & t \text{ has no edge in } T \text{ and an edge in } T' \end{cases}$$

This mapping is shown completely in Figure 9.

It is easy to see that $\mathcal{F}(\omega)$ is really a vertex configuration: Because every upward pointing triangle only borders downward pointing triangles, $\mathcal{F}(\omega)_{v_1}(e) = \mathcal{F}(\omega)_{v_2}(e)$ for each edge e and vertices v_1 and v_2 connected by e . From Figure 9 we also see that $\mathcal{F}(\omega)_v \in \mathcal{M}_v$ for all vertices v .

To see that \mathcal{F} is surjective, let $(\omega'_v)_v$ be a vertex configuration of the honeycomb constraint model. For each vertex v choose an edge configuration of the surrounding triangle on the kagome lattice such that the triangle gets mapped to ω'_v . From Figure 9 it is clear that this is possible. This results in an overall valid trimer configuration, because every vertex in the kagome lattice is now in exactly one trimer.

To see property 2), suppose ω and η are two edge configurations in the trimer constraint model. If $\mathcal{F}(\omega)_v = \mathcal{F}(\eta)_v$ for a vertex v , but $\omega(e) \neq \eta(e)$ on an edge on the triangle around v , then this triangle must be in one of the first three configurations in Figure 9

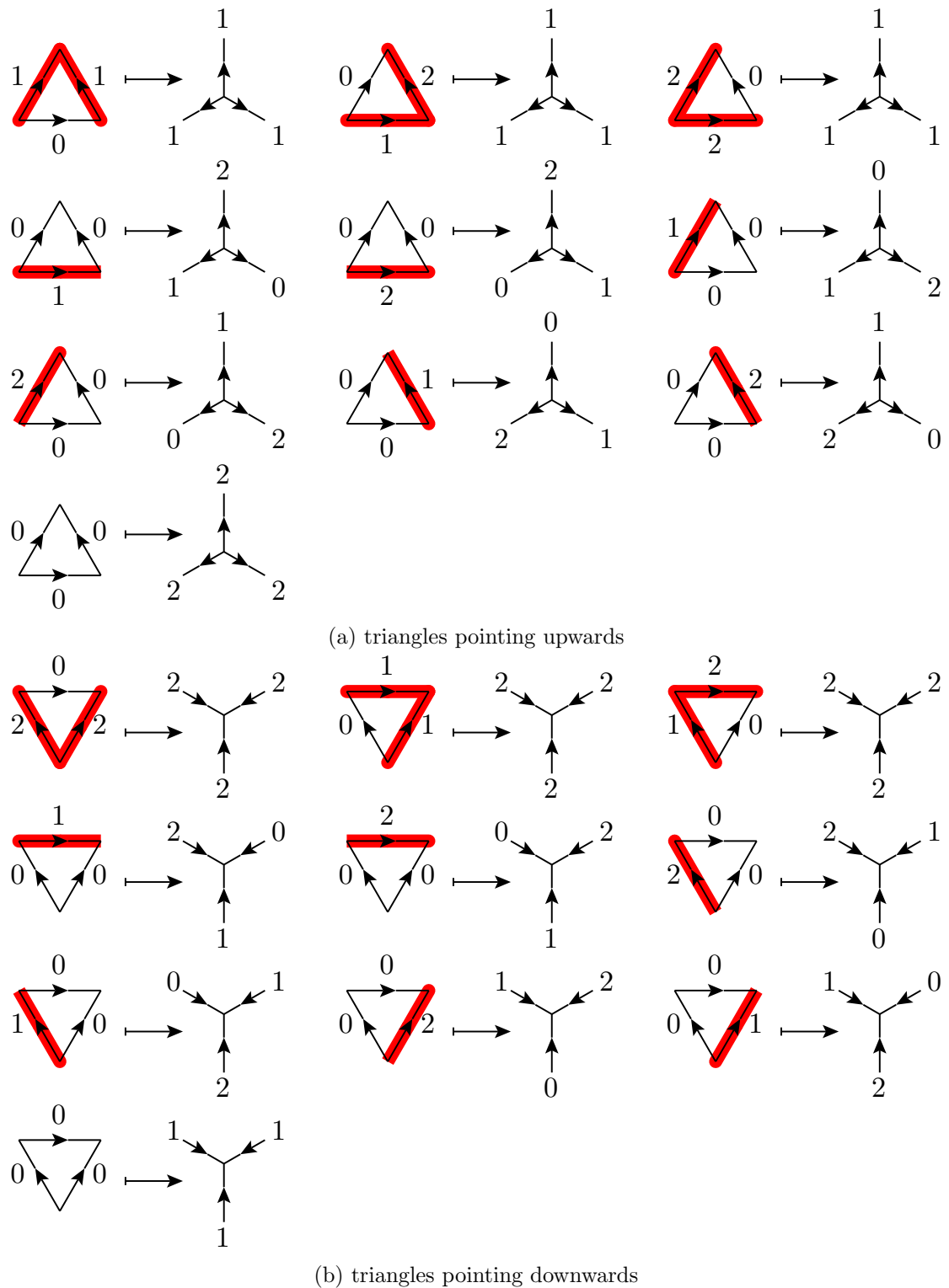
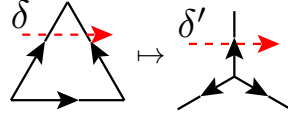


Figure 9: Mapping from a 3-perfect matching on the kagome lattice to a vertex configuration of the honeycomb constraint model. The numbers on the triangles show the edge configurations corresponding to the 3 perfect matching by Theorem 3.4

a) or b), because all other configurations get mapped to distinct $\mathcal{F}(\omega)_v$. But all of these three configurations can be transformed into each other using a local move with length 3.

To see property 3), note that if $\mathcal{F}(\omega)$ and $\mathcal{F}(\eta)$ differ on d edges, then by the above argument we can find ω' with $\mathcal{F}(\omega) = \mathcal{F}(\omega')$ such that ω' and η differ on at most $2d$ triangles. So ω' and η differ on at most $6d$ edges.

To see property 4), assume without loss of generality that γ only intersects upward pointing triangles. If γ intersects a downward pointing triangle, we can always perturb it such that it instead intersects an upward pointing triangle. Construct the path γ' by replacing path segments δ of γ by δ' like



on the top edge and similarly on the bottom left and bottom right edge on each triangle. It is easy to check that

$$\int_{\delta'} \mathcal{F}(\omega) = 1 + \int_{\delta} \omega$$

Note that you only have to check that on, say, the top edge, because on the other two edges it follows by symmetry. Then if $\int_{\gamma} \omega = \int_{\gamma} \eta$, it follows that $\int_{\gamma'} \mathcal{F}(\omega) = \int_{\gamma'} \mathcal{F}(\eta)$. \square

4.2 Blocking Tensors on the Honeycomb Lattice

The next Theorem will be the crucial step in proving that two trimer configurations on the kagome lattice with the same loop invariants can be transformed into each other using a chain of local moves. We show that any edge configuration on the boundary of one of the subgraphs in Figure 10 can be extended to a full edge configuration, as long as its integral along the boundary vanishes.

Theorem 4.2. *Let $G = (V, E)$ be the subgraph of the honeycomb lattice shown in Figure 10 a) and γ the path shown in that figure. Let B be the set of half edges of G . Let $\omega' : B \rightarrow \mathbb{Z}_3$ such that $\int_{\gamma} \omega' = 0$. Then there is a vertex configuration $(\omega_v)_{v \in V}$ in the honeycomb constraint model on G' such that $\omega_v(e) = \omega'(e)$ for $e \in B$ and v the vertex that e is connected to.*

Proof. Let us define a tensor similar to the tensor used to define the PEPS state, but omit the physical space. Attach

$$A_v = \sum_{\eta_v \in \mathcal{M}_v} \bigotimes_e \eta_v(e) \in \mathcal{H}_{virt}^{\otimes 3}$$

to each vertex v such that all edges at v start in v , where we take the tensor product over all these edges. Further, attach

$$A_v^* = \sum_{\eta_v \in \mathcal{M}_v} \bigotimes_e \eta_v(e)^* \in \mathcal{H}_{virt}^*{}^{\otimes 3}$$

to each vertex v such that all edges at v end in v .

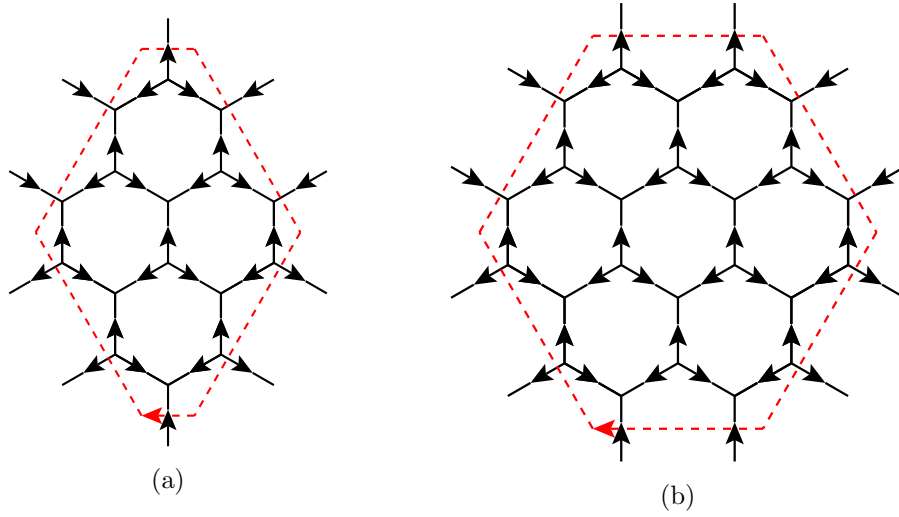


Figure 10: The two subgraphs of the honeycomb lattice we will consider in this section. When the integral of an edge configurations defined on the boundary around the dashed path γ is 0, it can be extended to a vertex configuration on the complete subgraph.

Consider the value $T \in \mathcal{H}_{virt}^{\otimes 5} \otimes \mathcal{H}_{virt}^* \otimes \mathcal{H}_{virt}^{\otimes 5}$ of this tensor network. It is easy to see that $\langle \bigotimes_{e \in B} \omega'(e), T \rangle$ is the number of vertex configurations $(\omega_v)_v$ such that $\omega_v(e) = \omega'(e)$ for $e \in B$ and v the vertex that e is connected to. We have to check that this number is positive whenever $\int_{\gamma} \omega' = 0$.

This is just a calculation, which can be done using a tensor network software. I used ITensor [16] for this purpose. We need to check $3^9 < 20000$ values of ω' which takes less than 1 second on a PC with an Intel[®] Core™ i5-3210M CPU and 8GB memory. \square

Because this proof extensively relies on a computer calculation, it does not provide much insight to the problem, nor is it feasible to generalize this proof to similar problems, like for tetramers on the kagome lattice. For this reason we will show the slightly weaker theorem, that Theorem 4.2 holds for Figure 10 b) instead, without computer use.

For this, we first need to define a derivative of a function from the faces of a lattice to an abelian group.

Definition 4.3 (Derivative on a Lattice). Let G be an abelian group and $f : F \rightarrow G$ a function, where F are the faces of a graph. Let E be the edges of the same graph. Then we define the derivative $df : E \rightarrow G$ to be $df(e) = f(F_L) - f(F_R)$ where $F_L, F_R \in F$ are the faces to the left and to the right of e .

Lemma 4.4. Let f like in Definition 4.3. Let F_1, F_2 be two faces of the lattice and γ a path between them. Then

$$\int_{\gamma} df = f(F_2) - f(F_1)$$

Proof. Let $\gamma = (G_0, G_1, \dots, G_n)$ ($n \in \mathbb{N}$) with faces G_0, \dots, G_n . It is $G_0 = F_1, G_n = F_2$. Then

$$\int_{\gamma} df = \sum_{i=1}^n f(G_i) - f(G_{i-1}) = f(G_n) - f(G_0)$$

\square

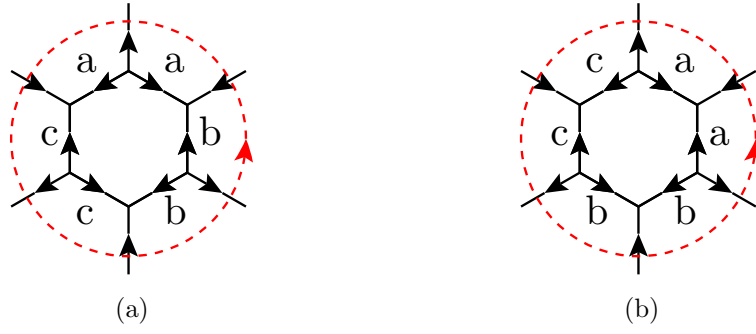


Figure 11: See Lemma 4.6

Lemma 4.5 (Poincare Lemma). *Let E' and F' be the edges and faces of a subgraph of a lattice, such that each path that lies completely in this subgraph has winding numbers $(0,0)$. Let $\omega : E' \rightarrow G$ be a function such that for each lattice v and the path ϵ encircling v $\int_{\epsilon} \omega = 0$. Then there is an $f : F' \rightarrow G$ such that $\omega = df$.*

Proof. For a closed path γ it is $\int_{\gamma} \omega = 0$, because we can find a homotopy from γ to a path that encircles a single vertex. Because $\int_{\epsilon} \omega = 0$ for each ϵ encircling a vertex, this homotopy does not change the value of the integral.

Now choose a face F_0 . For each face F let γ_F be a path from F_0 to F and set $f(F) = \int_{\gamma_F} \omega$. f is well defined, because for two paths γ_F and δ_F $\int_{\gamma_F} \omega = \int_{\delta_F} \omega$, because joining γ_F and the reverse of δ_F gives a closed path. Then $df = \omega$. \square

With these tools we can now first study the question for which ω' Theorem 4.2 fails if we use the subgraph of a single hexagon, as shown in Figure 11, instead of the subgraph in Figure 10 a).

Lemma 4.6. *Let (V, E) be the subgraph of a single hexagon, and denote by B the half edges of this subgraph. Denote by F_M the face of the hexagon itself. Let $\omega' : B \rightarrow \mathbb{Z}_3$ such that $\int_{\gamma} \omega' = 0$. Let F_0 be a face bordering F_M (one of the faces marked with a letter in Figure 11), and for any other of those faces F set $f(F) = \int_{\gamma_F} \omega'$, where γ_F is a segment of the path shown in Figure 11 from F_0 to F . Then we can extend f to F_M such that df is a vertex configuration in the honeycomb constraint model if and only if f is not of the form shown in Figure 11 a) or b) for some $a, b, c \in \mathbb{Z}_3$ with $\{a, b, c\} = \mathbb{Z}_3$.*

Proof. The only way that df is not a valid vertex configuration is that f assigns the same value to all three faces that share a vertex, because then $df(e) = 0$ for each edge e between two of these edges. Hence the only way we can't extend f is if for each $x \in \mathbb{Z}_3$ there are two bordering faces F_1 and F_2 each bordering F_M , and $f(F_1) = f(F_2) = x$. But this means f must look like in Figure 11 with $\{a, b, c\} = \mathbb{Z}_3$. \square

Now we can use this result from a single hexagon to prove that for the subgraph given by seven hexagons in Figure 10 b) any edge configuration on the boundary that integrates to 0 can be extended to a vertex configuration in the inside.

Theorem 4.7. *Theorem 4.2 also holds for the subgraph in Figure 10 b).*

Proof. Just like in Lemma 4.6 we can define a function $f(F) = \int_{\gamma_F} \omega'$ on the faces on the boundary of the subgraph such that for each $e \in B$, $\omega'(e) = df(e)$.

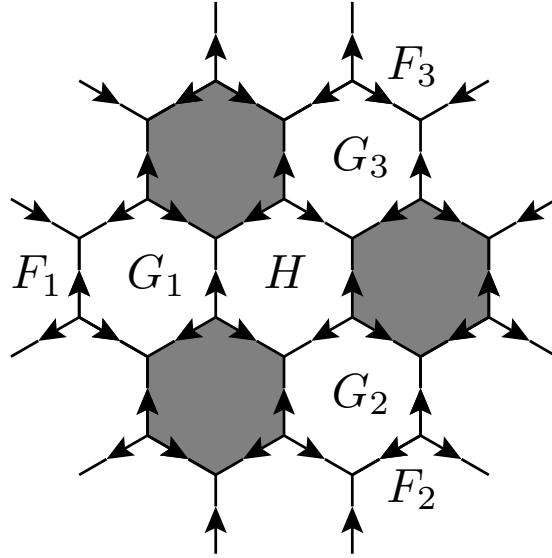


Figure 12: Any function f on the faced on the boundary of this subgraph can be extended to the whole subgraph such that df is a vertex configuration

Now consider the faces $F_1, F_2, F_3, G_1, G_2, G_3, H$ shown in Figure 12. Choose $f(G_i) = f(F_i) \pm 1$ for $i = 1, 2, 3$. Choose the sign in such a way that $f(G_i) \neq 0$ (If $f(F_i) = 0$ then both signs are possible, just choose any). Further, set $f(H) = 0$. By Lemma 4.6 we can extend f to the gray hexagons such that df is an vertex configuration on all vertices bordering one of the hexagons. The only vertices that do not border one of the gray hexagons are those connected by the edge between F_i and G_i for $i = 1, 2, 3$. But df is also a vertex configuration on these vertices, because $f(F_i) \neq f(G_i)$, and all we need to show is f does not map all faces on a vertex to the same value. Hence df is a vertex configuration. \square

Theorem 4.2 and Theorem 4.7 imply that the tensor we get by adding a half edge for each vertex (like when defining quantum states from tensor networks) is \mathbb{Z}_3 -injective, as defined in [13]. It was shown in [13] that \mathbb{Z}_3 -injective tensors on the square lattice yield parent Hamiltonians whose ground space is spanned by the states in Theorem 2.18. This implies that two N -mer vertex configurations with the same loop invariants can be transformed into each other by a chain of local moves. The proof in [13] holds in spirit also for the honeycomb lattice. However, in the next section we will show the same statement without using the theory of G -injective tensors.

4.3 From Honeycomb to Triangular Lattice

The subgraph in Figure 10 a) can be used to fill the whole N_x, N_y -honeycomb lattice for N_x divisible by 4 and N_y even, as shown in Figure 13. If we consider the graph in which these subgraphs are vertices and connected by an edge if the large hexagons in Figure 13 share an edge, we get the $N_x/4, N_y/2$ -triangular lattice. The same works for the subgraph in Figure 10 b) if N_x is divisible by 6 and N_y is even.

Let us define a simple *triangular constraint model* on the triangular lattice by

$$\mathcal{M}_v = \{\omega_v : E_v \rightarrow \mathbb{Z}_3 \mid \sum_{i=1}^6 (-1)^i \omega_v(e_i) = 0\}$$

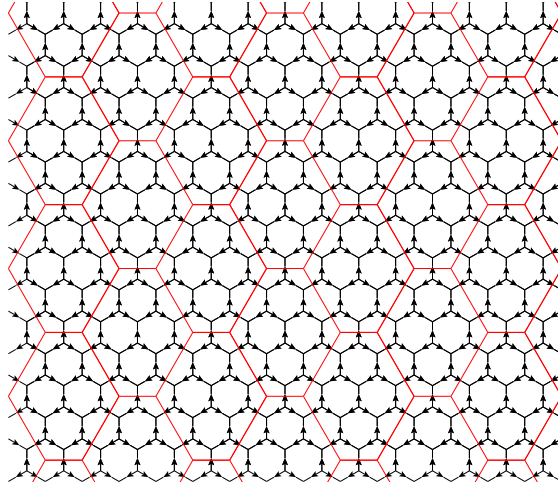


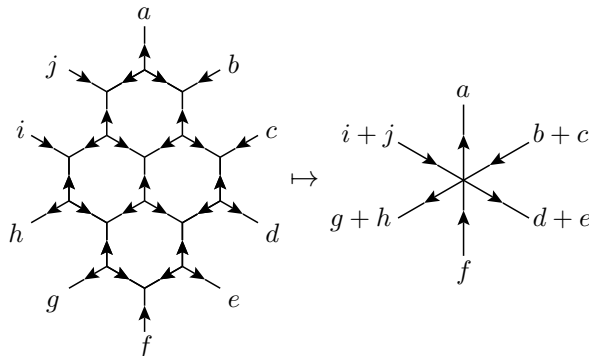
Figure 13: The subgraphs from Figure 10 can be used to fill the honeycomb lattice

where $E_v = \{e_1, \dots, e_6\}$ are the edges connected to v , which we enumerate counterclockwise. Edge configurations in this constraint model are exactly the maps $\omega : E \rightarrow \mathbb{Z}_3$ such that $\int_\epsilon \omega = 0$ when ϵ is a path encircling a single vertex. Similar to when going from the kagome to the honeycomb lattice, we can now find a mapping from the honeycomb to the triangular lattice which does not affect the loop invariants.

Theorem 4.8 (Map from Honeycomb to Triangular Lattice). *There is a map \mathcal{F} from vertex configurations in the N_x, N_y -honeycomb constraint model to the vertex configurations in the $N_x/4, N_y/2$ -triangular constraint model such that*

1. \mathcal{F} is surjective
2. If $\mathcal{F}(\omega) = \mathcal{F}(\eta)$ there is a chain of local moves of size at most 40 that transforms η to ω
3. If $\mathcal{F}(\omega)$ and $\mathcal{F}(\eta)$ differ on at most d vertices, then there is ω' which differs from η at at most $16d$ vertices such that $\mathcal{F}(\omega) = \mathcal{F}(\omega')$
4. For each path γ on the dual of the honeycomb lattice there is a path γ' on the dual of the triangular lattice such that if $\int_\gamma \omega = \int_\gamma \eta$ then $\int_{\gamma'} \mathcal{F}(\omega) = \int_{\gamma'} \mathcal{F}(\eta)$.

Proof. Let ω be an edge configuration in the honeycomb constraint model. Let e be an edge in the triangular lattice and v a vertex at this edge. This vertex corresponds to one of the subgraphs in Figure 13, and e to either one edge e_0 or two edges e_1 and e_2 on the honeycomb lattice. Set $\mathcal{F}(\omega)_v(e)$ to be $\omega(e_0)$ or $\omega(e_1) + \omega(e_2)$. In pictorial representation this mapping is given by



For a given vertex configuration ω' in the triangular constraint model, we can choose $\omega : B \rightarrow \mathbb{Z}_3$, where B are the edges that are not completely in a single subgraph, such that $\mathcal{F}(\omega) = \omega'$ (Note that \mathcal{F} only depends on the edges in B). By Theorem 4.2 we can extend ω to an edge configuration in the honeycomb constraint model, so \mathcal{F} is surjective.

To see property 2), let ω and η be two edge configurations in the honeycomb constraint model such that $\mathcal{F}(\omega) = \mathcal{F}(\eta)$. Let e be an edge on the triangular lattice. Either e corresponds to a single edge e_0 , or to two edges e_1 and e_2 on the honeycomb lattice. In the first case we have $\omega(e_0) = \mathcal{F}(\omega)(e) = \mathcal{F}(\eta)(e) = \eta(e_0)$, in the second case we get $\omega(e_1) + \omega(e_2) = \eta(e_1) + \eta(e_2)$. In this second case we can change η on e_1 and e_2 to the values of ω on these edges. Because this does not change the integral of η along the paths around the subgraphs connected by e_1 and e_2 , we can change the values of η on the interior of these two subgraphs in a way that we get a valid vertex configuration. This local move changes η on the edges e_1 and e_2 , as well as on the 19 full edges of each of the two subgraphs, so on a total of 40 edges. By repeating these local moves we can achieve that ω and η agree on all edges in B . Now we only have to change the full edges of each subgraph from the values of η to the values of ω . This is a local move of size at most 19 for each subgraph.

To see property 3), observe that if $\mathcal{F}(\omega)$ and $\mathcal{F}(\eta)$ differ on d vertices, the ω and η differ on at most d subgraphs in such a way that they can't be transformed into each other using a local move on this subgraph and an adjacent one. Each subgraph contains 16 vertices, so η can be transformed to a ω' by changing η on 16 vertices, where ω' can be transformed to ω using local moves on at most two adjacent subgraphs.

For property 4) note that γ can be perturbed such that it only intersects edges in B . Then take path γ' on the dual of the triangular path to be the path which cuts the edges which are associated with the edges cut by γ . Then clearly $\int_{\gamma} \omega = \int_{\gamma'} \mathcal{F}(\omega)$ \square

Now we can show that any two edge configurations ω and η in the triangular constraint model such that $\int_{\gamma} \omega = \int_{\gamma} \eta$ and $\int_{\delta} \omega = \int_{\delta} \eta$, where γ and δ are two paths with winding numbers $(1,0)$ and $(1,0)$, can be transformed into each other using a chain of local moves. This proof is very similar to the standard proof that the de-Rahm cohomology of the torus is \mathbb{R}^2 .

Theorem 4.9. *Let γ and δ be two paths on the dual of the N_x, N_y -triangular lattice with winding numbers $(0,1)$ and $(1,0)$. Let ω and η be two edge configurations in the triangular constraint model. If $\int_{\gamma} \omega = \int_{\gamma} \eta$ and $\int_{\delta} \omega = \int_{\delta} \eta$, then there is a chain of local moves of size 3 that transforms ω to η*

Proof. First we will show that $\omega - \eta = df$ for some f . We can cover the N_x, N_y -triangular lattice by 4 subgraphs G_1, G_2, G_3, G_4 such that all paths that are completely in G_i for an $i \in \{1, 2, 3, 4\}$ have winding numbers $(0,0)$. To do this, let G_i be the subgraph with the vertices in $U_i \subseteq \mathbb{T}_{r,s}$ with $U_1 = (-0.1r, 0.6r) \times (-0.1s, 0.6s)$, $U_2 = (-0.1r, 0.6r) \times (0.6s, 1.1s)$, $U_3 = (0.6r, 1.1r) \times (-0.1s, 0.6s)$ and $U_4 = (0.6r, 1.1r) \times (0.6s, 1.1s)$. By Lemma 4.5 we can find functions f_i on the faces of G_i such that $\omega - \eta = df_i$ on all edges in G_i . Now G_1 and G_2 intersect in subgraphs H_{12} and H'_{12} , and there are constants C_{12} and C'_{12} such that $f_1 = f_2 + C_{12}$ on all faces of H_{12} and $f_1 = f_2 + C'_{12}$ on all faces of H'_{12} . Without loss of generality we can assume $C_{12} = 0$, because changing f_2 by a constant does not change df_2 . But because $\int_{\gamma} (\omega - \eta) = 0$ we get that also $C'_{12} = 0$. By the same arguments for the other subgraphs we get that $f_i = f_j$ on all faces which are in G_i and G_j . Hence there is a function f such that $\omega - \eta = df$ everywhere.

Now we can find functions f_0, f_1, \dots, f_n for an $n \in \mathbb{N}$ such that $f_0 = f$, $f_n = 0$ and f_i and f_{i+1} differ on only a single face for $i = 0, \dots, n-1$. Then $\rho_i = \eta + df_i$ is a valid edge configuration, because for each path ϵ encircling a vertex $\int_\epsilon \eta = 0$ because η is a valid edge configuration, and $\int_\epsilon df = 0$, because ϵ is a closed path. Now $\rho_0 = \omega$ and $\rho_n = \eta$, and ρ_i and ρ_{i+1} differ only on the 3 edges of the face on which f_i and f_{i+1} differ. Hence we have found a chain of local moves of size 3 from ω to η . \square

Now we can prove the main Theorem of this section:

Theorem 4.10. *There is a $D \in \mathbb{N}$ such that the following holds for all N_x divisible by 4 and N_y even: Let ω and η be two edge configurations in the trimer constraint model on the N_x, N_y -kagome lattice. Let γ and δ two paths with winding numbers $(1,0)$ and $(0,1)$ such that $\int_\gamma \omega = \int_\gamma \eta$ and $\int_\delta \omega = \int_\delta \eta$. Then there is a chain of local moves of size at most D that transforms ω to η .*

Proof. By the mappings from kagome to honeycomb lattice (Theorem 4.1) and from honeycomb to triangular lattice (Theorem 4.3) we can find edge configurations of the triangular constraint model ω' and η' such that there is a chain ρ_0, \dots, ρ_n of local moves of size 3 transforming ω' and η' . But because the maps in Theorem 4.1 and Theorem 4.3 are surjective, each ρ_i corresponds to an edge configuration in the trimer constraint model. By the above theorems, these edge configurations can be transformed into each other using a chain of local moves.

ρ_i and ρ_{i+1} differ on at most 3 vertices, so the corresponding vertex configurations on the honeycomb lattice differ on at most $3 \cdot 16 = 48$ vertices, up to local moves of size 40. Now the corresponding vertex configurations on the kagome lattice differ on at most $3 \cdot 48 = 144$ edges. Hence $D = 144$ satisfies the theorem. \square

The Theorem certainly also holds for smaller values of D , however, the exact value of D is not significant. Instead Theorem 4.10 implies that if we make the number of vertices in each term of the parent Hamiltonian large enough (but fixed in system size), the ground space dimension is exactly 9. From the proof of Theorem 4.9 we see that this depends on the genus, i.e. the dimension of the first de-Rahm cohomology, of the surface the state lives on. For a general surface with genus g the ground state is 3^g -fold degenerate.

4.4 Topological Order

4.4.1 A Simple Example

Since the trimer state on the kagome lattice has a ground state degeneracy depending on the genus of the surface, it is a candidate for topological order. We say a state ψ possesses *long range entanglement* or *topological order*, as defined in [17], if there is another state $\tilde{\psi}$ such that any local operator O looks like a multiple of the identity on the space spanned by ψ and $\tilde{\psi}$, up to an error decaying exponentially in the system size. This means that for a state on the N, N -lattice and any local operator O

$$|\langle \psi, O\psi \rangle - \langle \tilde{\psi}, O\tilde{\psi} \rangle| \leq C \exp(-aN) \quad (4)$$

and

$$|\langle \psi, O\tilde{\psi} \rangle| \leq C \exp(-aN) \quad (5)$$

for some constants C and a .

Why this property is called long range entanglement can be seen from a theorem proven in [17]: Let ψ be a state on a N, N -lattice. It can always be obtained from a direct product state ψ_0 via time evolution of some Hamiltonian H , i.e. $\psi = \exp(-iHt)\psi_0$, where H is local and does not depend on N [18]. Then if ψ posses long range entanglement, t scales linearly with N , while otherwise t converges to some constant for $N \rightarrow \infty$.

It has been argued in [19] that for states with topological order the number of the "brother" states $\tilde{\psi}$, and thus the degeneracy of the parent Hamiltonian, as the parent Hamiltonian is just a sum of local operators, depends on the genus of the surface the state lives on. However, we will soon see that the converse does not hold. A good review of topological order can be found in the first sections of [20].

To check whether a state exhibits topological order, we can study the largest few eigenvalues of the transfer operator. This is a common method, for example applied in [21] to a modified version of the toric code. We will now motivate it: A simple model on the honeycomb lattice with posses topological order can be defined similarly to the arguably most famous topological model, the toric code (defined in [5]). Define the *Gauss law constraint model* on the honeycomb lattice as

$$\mathcal{M}_v = \{\omega_v : E_v \rightarrow \mathbb{Z}_3 \mid \sum_{e \in E_v} \omega_v(e) = 0\}$$

Like the honeycomb constraint model defined earlier, this model has loop invariants given by $\int_\gamma \omega$ and $\int_\delta \omega$, where γ and δ are closed paths with winding numbers (1,0) and (0,1). Now let

$$\psi_{n,m} = \sum_{\substack{(\omega_v)_v \\ \int_\gamma \omega = n, \int_\delta \omega = m}} \bigotimes_{v \in V} \omega_v$$

be the equal superposition of all vertex configurations with a loop invariant n along γ and m along δ . We will show that the $\{\psi_n\}$ satisfy the equations (4) and (5), even with $C = 0$.

Equation (5) is immediately obvious, because no local move can change the loop invariants, so $\langle \psi_{n',m'}, O\psi_{n,m} \rangle = 0$ for any local operator O whenever $(n, m) \neq (n', m')$. To see (4), let O be a local operator which acts nontrivially only on a few vertices $\Omega \subseteq V$. Denote by Ω^c all other vertices and by B the set of edges between Ω and Ω^c . Then O is a superposition of

$$O_{\omega,\eta} = \sum_{\substack{(\rho_v)_{v \in \Omega^c} \\ \forall b \in B \rho(b) = \omega(b) = \eta(b)}} \left(\bigotimes_{v \in \Omega} \omega_v \otimes \bigotimes_{v \in \Omega^c} \rho_v \right) \otimes \left(\bigotimes_{v \in \Omega} \eta_v \otimes \bigotimes_{v \in \Omega^c} \rho_v \right)^*$$

with $(\omega_v)_{v \in \Omega}$ and $(\eta_v)_{v \in \Omega}$ such that $\forall b \in B \omega(b) = \eta(b)$. Now we see that

$$\langle \psi_{n,m}, O_{\omega,\eta} \psi_{n,m} \rangle = \left| \left\{ (\rho_v)_{v \in \Omega^c} \mid \forall b \in B \rho(b) = \omega(b) = \eta(b), \int_\gamma \rho = n, \int_\delta \rho = m \right\} \right|$$

where the integrals only depend on ρ because we can perturb γ and δ such that they do not intersect Ω .

Now let $\rho_{n,m}$ be an edge configuration on Ω^c such that $\forall b \in B \rho_{n,m}(b) = \omega(b) = \eta(b)$ and $\int_\gamma \rho_{n,m} = n$ and $\int_\delta \rho_{n,m} = m$. Because all paths in Ω have winding numbers (0,0),

and on vertices that correspond to downward pointing triangles

$$\alpha(\omega_v) = \begin{cases} \sqrt{3} & \text{if } \omega_v(e_1) = \omega_v(e_2) = \omega_v(e_3) = 2 \\ 0 & \text{if } \omega_v(e_1) = \omega_v(e_2) = \omega_v(e_3) = 0 \\ 1 & \text{otherwise} \end{cases}$$

The mapping in Figure 9 from kagome to honeycomb lattice shows that indeed this state is related to the quantum trimer state on the kagome lattice by a local unitary transformation. This transformation is given on the upward pointing triangles by

$$\begin{array}{c} 1 \\ | \\ \swarrow \quad \searrow \\ 1 \quad 1 \end{array} \mapsto \frac{1}{\sqrt{3}} \left(\begin{array}{c} \color{red}{\triangle} \\ \color{red}{\rightarrow} \end{array} + \begin{array}{c} \color{red}{\triangle} \\ \color{red}{\leftarrow} \end{array} + \begin{array}{c} \color{red}{\triangle} \\ \color{red}{\rightarrow} \end{array} \right)$$

and by mapping any other ω_v to the unique trimer configuration of the corresponding triangle. For this state we used the transfer operator

$$T = \dots \begin{array}{c} \uparrow \quad \uparrow \quad \uparrow \quad \uparrow \\ \swarrow \quad \searrow \quad \swarrow \quad \searrow \\ \uparrow \quad \uparrow \quad \uparrow \quad \uparrow \\ \swarrow \quad \searrow \quad \swarrow \quad \searrow \\ \uparrow \quad \uparrow \quad \uparrow \quad \uparrow \end{array} \dots$$

which is the square of the transfer operator given by equation (6). The values of the individual tensors are given by

$$\begin{array}{c} a \\ | \\ \swarrow \quad \searrow \\ b \quad c \end{array} = |\alpha(\omega_v)|^2$$

where $\omega_v(e_1) = a$, $\omega_v(e_2) = b$ and $\omega_v(e_3) = c$.

To understand whether the state exhibits topological order, have to check if a phase transition occurs when changing the $\alpha(\omega_v)$. A phase transition implies a diverging correlation length, and this in turn means that a gap needs to open between the three largest

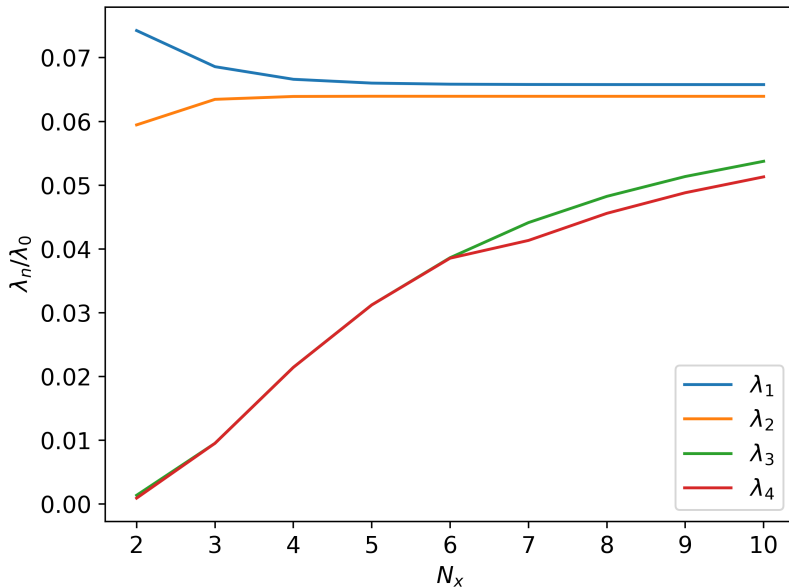


Figure 14: Ratio between second, third, fourth and fifth and the first eigenvalue of the transfer operator

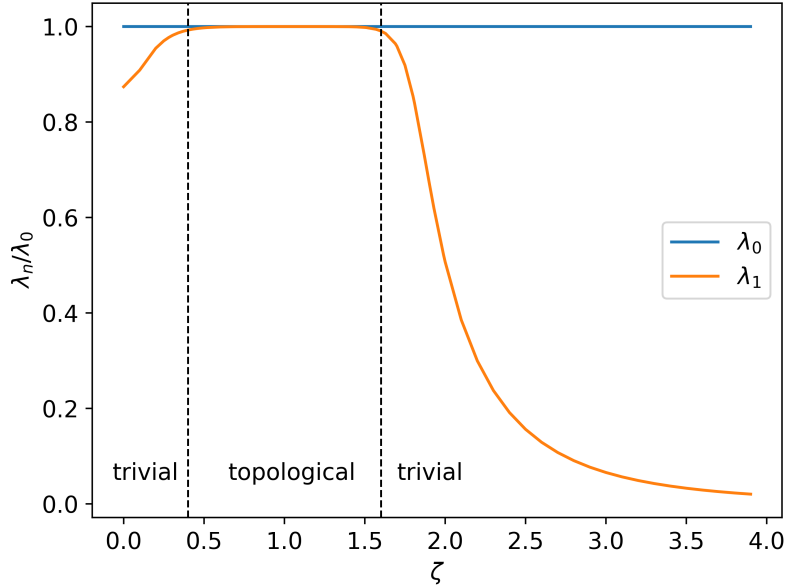


Figure 15: Gap between largest and second largest eigenvalue for different values of ζ . The third largest eigenvalue is always identical to the second largest eigenvalue, and therefore not shown here. We observe topological order for approximately $0.4 < \zeta < 1.6$

eigenvalues of the transfer operator. Hence we can check whether a phase transition has occurred by looking at the first three eigenvalues: If they are still the same in the limit $N_x \rightarrow \infty$, as they are for the Gauss law constraint model, we are still in the topological phase. If instead there is a gap between these eigenvalues, the state does not exhibit topological order anymore.

The ratios λ_n/λ_0 , where $|\lambda_0| \geq |\lambda_1| \geq |\lambda_2| \geq \dots$ are the eigenvalues of the transfer operator ordered by their modulus, are shown for different values of N_x in Figure 14. The eigenvalues of the transfer operator were computed using the Arnoldi Iteration algorithm [22] and the ITensor software package [16]. This computation suggests that for $N_x \rightarrow \infty$ there is a gap between the largest and the second and third largest eigenvalue of the transfer operator, with $\lambda_2 \approx \lambda_1 \approx 0.07\lambda_0$. This implies that the quantum trimer state on the kagome lattice does not exhibit topological order.

However, we can change our model slightly such that it exhibits topological order. To do this, we define new weights depending on a parameter $\zeta \in \mathbb{R}$ by

$$\alpha(\omega_v) = \begin{cases} \zeta^{1/2} & \text{if } \omega_v(e_1) = \omega_v(e_2) = \omega_v(e_3) = 1 \\ 0 & \text{if } \omega_v(e_1) = \omega_v(e_2) = \omega_v(e_3) = 0 \\ 1 & \text{otherwise} \end{cases}$$

for vertices corresponding to upward pointing triangles, and

$$\alpha(\omega_v) = \begin{cases} \zeta^{1/2} & \text{if } \omega_v(e_1) = \omega_v(e_2) = \omega_v(e_3) = 2 \\ 0 & \text{if } \omega_v(e_1) = \omega_v(e_2) = \omega_v(e_3) = 0 \\ 1 & \text{otherwise} \end{cases}$$

for vertices corresponding to downward pointing triangles. For $\zeta = 3$ this is the quantum trimer model on the kagome lattice.

The ratio between the largest and the second largest eigenvalue at $N_x = 10$ is plotted for different values of ζ in Figure 15. Examining the eigenvalues for increasing values of N_x at different, fixed values of ζ shows that the second eigenvalue is always converged at $N_x = 10$, except close to $\zeta = 0.4$ and $\zeta = 1.6$. We see that for approximately $0.4 < \zeta < 1.6$ there is no gap between the eigenvalues, which implies that the model is topological in that region.

There is a convenient interpretation of the parameter ζ : From the mapping from kagome to honeycomb lattice in Figure 9 we see that we get a weight of $\zeta^{1/2}$ at a vertex in the honeycomb lattice if there is a trimer lying completely in the triangle on the kagome lattice corresponding to that vertex. Hence the state given by the $\alpha(\omega_v)$ is related by a local unitary transformation to the superposition of all trimer coverings of the kagome lattice, where we weight each configuration with $(\zeta/3)^{M/2}$ and M is the number of trimers that lie completely in a single triangle of the kagome lattice.

5 The Dimer Model on the Square Lattice

In this section we will study the degeneracy of the parent Hamiltonian describing the dimer model on the square lattice. We already saw in section 3.3 that there are two loop invariants with values in \mathbb{Z} that remain unchanged under local moves. It has been conjectured in [14] that any two vertex configurations with the same loop invariants can be transformed into each other using a chain of local moves. Even though we won't prove this conjecture, we will give a different view onto the problem which makes the conjecture seem very intuitive.

We want to map a vertex configuration in the dimer model to a configuration of oriented loops on the torus. For this, we define the *oriented loop constraint model* on the N_x, N_y -square lattice to be the constraint model given by

$$\mathcal{M}_v = \{ \omega_v : \{f_1, f_2, f_3, f_4\} \rightarrow \{-1, 0, 1\} \mid \omega_v(f_1) - \omega_v(f_2) - \omega_v(f_3) + \omega_v(f_4) = 0 \text{ and not } [\omega_v(f_1) = \omega_v(f_3) \in \{-1, 1\} \text{ and } \omega_v(f_2) = \omega_v(f_4) \in \{-1, 1\}] \}$$

where f_1, \dots, f_4 are the edges in Figure 16 a). Thus, ω is an edge configuration in the oriented loop constraint model if and only if $\int_\epsilon \omega = 0$ for all paths ϵ encircling a single vertex and if not both pairs of opposite edges get mapped to the same value in $\{-1, 1\}$.

We want to call this the oriented loop constraint model because of the following interpretation: Consider an edge configuration ω . For an edge f with $\omega(f) \neq 0$ assign a direction to f . Set this direction to be the inherent direction of f on the lattice when $\omega(f) = 1$, and the opposite direction if $\omega(f) = -1$. Examples for this interpretation are given in Figure 16 b)-d). Let N_{in} be the number of edges that point towards this vertex in this new direction, and N_{out} the number of edges that point away from the vertex. Then $0 = \omega(f_4) + \omega(f_1) - \omega(f_2) - \omega(f_3) = N_{out} - N_{in}$. Hence the edges with $\omega(f)$ form closed loops, and each loop has a consistent orientation.

From the definition of the oriented loop constraint model it is easy to see that $\omega_v \in \mathcal{M}_v$ whenever the same number of edges enter v as there are edges leaving. The only exception is given in Figure 16 e), and all rotations of the red configuration. This exception can be interpreted as the constraint that two oriented loops are not allowed to intersect. Not that however a "touching" of two oriented loops as in Figure 16 d) is permitted.

Because $\int_\epsilon \omega = 0$ for all edge configurations and ϵ a path encircling a single vertex, we get a two loop invariants given by $\int_\gamma \omega$ and $\int_\delta \omega$ for closed paths γ and δ with winding numbers (1,0) and (0,1) respectively. The value of these invariants is exactly given by $N_{LR} - N_{RL}$ where N_{LR} is the number of times γ or δ is intersected from the left to the right, and N_{RL} is the number of intersections from right to left. Hence the invariants are just given by the sum of the winding numbers of all oriented loops.

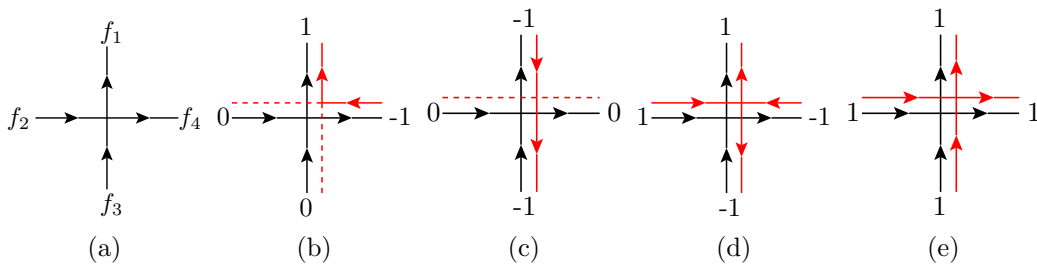


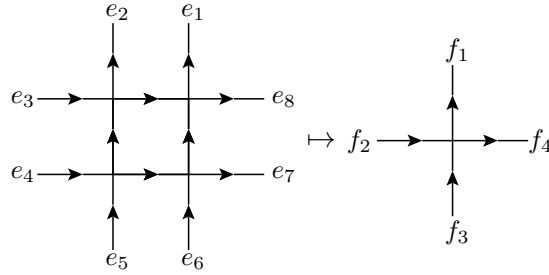
Figure 16: (a) Labeling of the edges in oriented loop constraint model, (b)-(d) Allowed configuration in oriented loop constraint model, (e) Forbidden configuration

Now we will show that we can map a vertex configuration in the dimer constraint model to a vertex configuration in the oriented loops constraint mapping such that the loop invariants are preserved:

Theorem 5.1. *Let N_x and N_y be even. There is a map \mathcal{F} from the vertex configurations in the dimer constraint model on the N_x, N_y -square lattice to the vertex configurations in the oriented loop constraint model on the $N_x/2, N_y/2$ -square lattice such that*

1. \mathcal{F} is surjective
2. If $\mathcal{F}(\omega) = \mathcal{F}(\eta)$ then ω and η can be transformed into each other by a chain of local moves of size 4
3. If $\mathcal{F}(\omega)$ and $\mathcal{F}(\eta)$ differ on at most d vertices, then there is ω' such that $\mathcal{F}(\omega) = \mathcal{F}(\omega')$ and ω' and η differ on at most $4d$ vertices
4. For each closed path γ on the dual of the N_x, N_y -square lattice there is a path γ' on the dual of the $N_x/2, N_y/2$ -square lattice such that for all dimer configurations ω and η with $\int_\gamma \tilde{\omega} = \int_\gamma \tilde{\eta}$ it holds that $\int_{\gamma'} \mathcal{F}(\omega) = \int_{\gamma'} \mathcal{F}(\eta)$. Here, $\tilde{\omega}$ is the map from the edges of the square lattice to \mathbb{Z} that yields the \mathbb{Z} invariant in section 3.3.

Proof. Let ω be an edge configuration in the dimer constraint model. We get an edge configuration on the oriented loop model by mapping quadruples of vertices on the N_x, N_y -square lattice to a single lattice on the $N_x/2, N_y/2$ -square lattice like



and setting

$$\begin{aligned}\mathcal{F}(\omega)(f_1) &= \omega(e_1) - \omega(e_2) \\ \mathcal{F}(\omega)(f_2) &= -\omega(e_3) + \omega(e_4) \\ \mathcal{F}(\omega)(f_3) &= -\omega(e_5) + \omega(e_6) \\ \mathcal{F}(\omega)(f_4) &= \omega(e_7) - \omega(e_8)\end{aligned}$$

Then

$$\begin{aligned}\mathcal{F}(\omega)(f_1) - \mathcal{F}(\omega)(f_2) - \mathcal{F}(\omega)(f_3) + \mathcal{F}(\omega)(f_4) &= \\ \omega(e_1) - \omega(e_2) - \omega(e_3) + \omega(e_4) + \omega(e_5) - \omega(e_6) - \omega(e_7) + \omega(e_8) &= \int_\gamma \tilde{\omega} = 0\end{aligned}$$

Where γ is the path on the dual of the N_x, N_y -square lattice encircling all four vertices.

Further, suppose it would be $\mathcal{F}(\omega)(f_1) = \mathcal{F}(\omega)(f_3) = 1$ and $\mathcal{F}(\omega)(f_2) = \mathcal{F}(\omega)(f_4) = 1$. Then $\omega(e_6) = \omega(e_7) = 1$, so ω cannot be an edge configuration in the dimer constraint model. With analogous arguments we can exclude the cases $\mathcal{F}(\omega)(f_1) = \mathcal{F}(\omega)(f_3) = -\mathcal{F}(\omega)(f_2) = -\mathcal{F}(\omega)(f_4) = 1$, $-\mathcal{F}(\omega)(f_1) = -\mathcal{F}(\omega)(f_3) = \mathcal{F}(\omega)(f_2) = \mathcal{F}(\omega)(f_4) = 1$ and $-\mathcal{F}(\omega)(f_1) = -\mathcal{F}(\omega)(f_3) = -\mathcal{F}(\omega)(f_2) = -\mathcal{F}(\omega)(f_4) = 1$. Hence $\mathcal{F}(\omega)$ is indeed an edge configuration in the oriented loop constraint model.

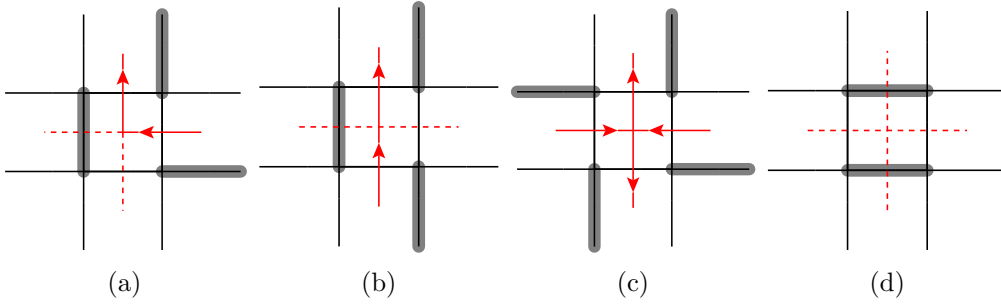
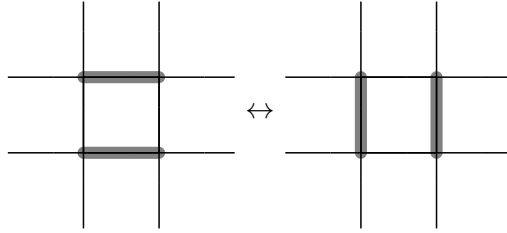


Figure 17: Map from oriented loop model to dimer constraint model showing that \mathcal{F} is surjective

To see that \mathcal{F} is surjective choose for a vertex configuration $(\omega'_v)_v$ in the oriented loop constraint model and for a vertex v a vertex configuration in the dimer model as shown in Figure 17. Up to symmetry all elements of \mathcal{M}_v are shown in Figure 17. The resulting vertex configuration ω in the dimer constraint model is a valid vertex configuration and satisfies $\mathcal{F}(\omega) = \omega'$.

To see property 2, suppose that $\mathcal{F}(\omega) = \mathcal{F}(\eta)$. Suppose $\omega(e) \neq \eta(e)$ for an edge e which is one of the edges e_1, \dots, e_8 for some vertex in the above mapping. Then there is a neighboring edge e' such that $\omega(e) - \omega(e') = \eta(e) - \eta(e')$. Let w.l.o.g. $\omega(e) = \omega(e') = 1$ and $\eta(e) = \eta(e') = 0$, the other possibility would be the same with ω and η interchanged. Then we can make ω and η agree by doing the local move



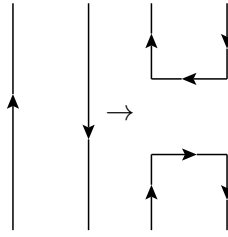
where e and e' are two of the parallel edges. This local move has size 4. Now suppose ω and η agree on all edges e_1, \dots, e_8 for some quadruple of vertices. Then we can make them also agree on the four edges connecting two vertices from this quadruple by a local move of size 4.

Property 3 is obvious from the definition of \mathcal{F} .

For property 4 perturb the path γ such that it only intersects edges that correspond to the edges e_1, \dots, e_8 for some vertex. Choose γ' to be the corresponding path on the $N_x/2, N_y/2$ -square lattice we get by cutting an edge f_i whenever γ cuts e_{2i-1} and e_{2i} for $i = 1, \dots, 4$. Then $\int_{\gamma'} \tilde{\omega} = \int_{\gamma} \mathcal{F}(\omega)$. \square

Now the original conjecture is equivalent to the conjecture that any two configurations of oriented loops on the torus with the same winding numbers can be transformed into each other by a chain of local moves. We won't prove this conjecture, but at least make it plausible: Given an oriented loop with winding numbers $(0,0)$, we can shrink it away by local moves. Hence, whether two configurations can be transformed into each other should only depend on the winding numbers of the loops in these configurations. Note that two loops which wind around the torus in different direction (i.e. the winding numbers are the negative of each other) can be transformed to the empty torus by first

doing local moves like



to change them to loops with winding numbers $(0,0)$, and then shrinking these loops away. Hence whether two configurations can be transformed into each other should not depend on the winding numbers of the individual loops, but only on their sum.

6 Conclusion

In this thesis I studied quantum N -mer models. In Theorem 3.4 I showed how any N -mer model can be described by a constraint model, which in turn describes a PEPS. In Theorem 3.5 I proved that the ground states of the parent Hamiltonian of a quantum N -mer model are given by superpositions of all N -mer coverings of the lattice, where two coverings must have the same amplitude when they can be transformed into each other using a chain of local moves.

In section 4 I then gave a proof that two trimer coverings on the kagome lattice can be transformed into each other using a chain of local moves if and only if their integrals around two paths with winding numbers $(1,0)$ and $(0,1)$ are equal. This implies that the ground space of the parent Hamiltonian of the trimer model has dimension 9. The idea of this proof was to first map the trimer coverings on the kagome lattice to a different model on the honeycomb lattice. If we block enough sites on the honeycomb lattice together, any edge configuration on the boundary of a certain subgraph which integrates to zero along that boundary can be extended to a complete edge configuration. This was shown in Theorem 4.2 largely relying on a computation done using a computer, and in Theorem 4.7 without computer use. Using this result, the model on the honeycomb lattice can be mapped to a simple model on the triangular lattice. On this lattice the claim can then easily be shown. In section 4.4 I also gave numerical evidence that the trimer model on the kagome lattice does not exhibit topological order. I proposed a similar model which does exhibit topological order

In section 5 I showed that the quantum dimer model on the square lattice is equivalent to the model of oriented loops. The conjecture that two dimer configurations with the same loop invariants can be transformed into each other using a chain of local moves appears more plausible in the model of oriented loops.

The field of quantum N -mer models still holds many interesting questions. Numerical evidence in [6] suggests that also the trimer model on the square lattice should have a 9 dimensional ground space. However, no rigorous proof of this statement is known. It is also unclear whether the analysis of the trimer model on the kagome model can be extended to the tetramer model on the kagome lattice. Computations similar to those in Theorem 4.2 suggest that this might be possible if enough sites are blocked together. It is also an interesting question how to generalize the statements that apply only to the N_x, N_y -kagome lattice when N_x is divisible by 4 and N_y even to general values of N_x and N_y .

References

- [1] Ernst Ising. Beitrag zur Theorie des Ferromagnetismus. *Zeitschrift für Physik*, 31(1):253–258, Feb 1925.
- [2] Daniel S. Rokhsar and Steven A. Kivelson. Superconductivity and the quantum hard-core dimer gas. *Phys. Rev. Lett.*, 61:2376–2379, Nov 1988.
- [3] R Moessner and Lakshman Sondhi. Resonating valence bond phase in the triangular lattice quantum dimer model. *Physical review letters*, 86:1881–4, 03 2001.
- [4] Xiao-Gang Wen. Topological orders in rigid states. *Int. J. Mod. Phys. B*, 4:239, 01 1990.
- [5] A Yu. Kitaev. Fault-tolerant quantum computation by anyons. *Annals of Physics*, 303, 01 2003.
- [6] Hyun-Yong Lee, Yun-tak Oh, Jung Hoon Han, and Hosho Katsura. Resonating valence bond states with trimer motifs. *Physical Review B*, 95:060413, 02 2017.
- [7] Ulrich Schollwöck. The density-matrix renormalization group in the age of matrix product states. *Annals of Physics*, 326(96), 2011.
- [8] Guifré Vidal. Efficient classical simulation of slightly entangled quantum computations. *Phys. Rev. Lett.*, 91:147902, Oct 2003.
- [9] Jacob C Bridgeman and Christopher T Chubb. Hand-waving and interpretive dance: an introductory course on tensor networks. *Journal of Physics A: Mathematical and Theoretical*, 50(22):223001, may 2017.
- [10] Roman Orus. A practical introduction to tensor networks: Matrix product states and projected entangled pair states. *Annals of Physics*, 349, 06 2013.
- [11] M B. Hastings. An area law for one dimensional quantum systems. *Journal of Statistical Mechanics Theory and Experiment*, 2007, 05 2007.
- [12] M B. Hastings. Solving gapped hamiltonians locally. *Physical Review B*, 73, 08 2005.
- [13] Norbert Schuch, Ignacio Cirac, and David Pérez-García. Peps as ground states: Degeneracy and topology. *Annals of Physics*, 325:2153–2192, 01 2010.
- [14] R Moessner and K.S. Raman. *Introduction to Frustrated Magnetism*, volume 164 of *Springer Series in Solid-State Sciences*, chapter Quantum Dimer Models. Springer, Berlin, Heidelberg, 2011.
- [15] Norbert Schuch, Didier Poilblanc, J Ignacio Cirac, and David Perez-Garcia. Resonating valence bond states in the peps formalism. *Physical Review B*, 86, 03 2012.
- [16] *ITensor Library (version 2.0.11)* <http://itensor.org>.
- [17] S Bravyi, M B Hastings, and Frank Verstraete. Lieb-robinson bounds and the

- generation of correlations and topological quantum order. *Physical review letters*, 97:050401, 09 2006.
- [18] Michael A. Nielsen and Isaac L. Chuang. *Quantum Computation and Quantum Information: 10th Anniversary Edition*. Cambridge University Press, 2010.
- [19] Alexei Kitaev and John Preskill. Topological entanglement entropy. *Phys. Rev. Lett.*, 96:110404, Mar 2006.
- [20] Xie Chen, Zheng Cheng, and Xiao-Gang Wen. Local unitary transformation, long-range quantum entanglement, wave function renormalization, and topological order. *Physical Review B*, 82, 04 2010.
- [21] Norbert Schuch, Didier Poilblanc, J Ignacio Cirac, and David Perez-Garcia. Topological order in peps: Transfer operator and boundary hamiltonians. 10 2012.
- [22] Yousef Saad. *Numerical Methods for Large Eigenvalue Problems*, volume 66. 01 1992.

Acknowledgments

I would first like to thank Prof. Dr. Norbert Schuch of the Max Planck Institute of Quantum Optics (MPQ) for supervising this thesis and for the many useful discussions. I would like to thank Dr. Mohsin Iqbal of MPQ for answering every single one of my questions and for his valuable feedback while I was writing this thesis. I would like to thank Prof. Dr. Jan von Delft of LMU for being my formal supervisor in the faculty of physics. I would like to thank Prof. Dr. Phan Thành Nam for being my formal supervisor in the department of mathematics and for the useful feedback and discussions. I would like to thank my friend Edward Wang for proofreading this thesis.

Selbstständigkeitserklärung

Hiermit erkläre ich, die vorliegende Arbeit selbständig verfasst zu haben und keine anderen als die in der Arbeit angegebenen Quellen und Hilfsmittel benutzt zu haben.

München, den 06. Juni 2019

Sven Jandura